Supporting Information

Scandium bis(trimethylsilyl)methyl complexes revisited: extending the ^{45}Sc NMR chemical shift range and a new structural motif of Li[CH(SiMe$_3$)$_2$]

Alexandros Mortis, Damir Barisic, Klaus Eichele, Cäcilia Maichle-Mössmer, and Reiner Anwander*

Institut für Anorganische Chemie, Eberhard Karls Universität Tübingen, Auf der Morgenstelle 18, 72076 Tübingen, Germany

*E-mail for R. A.: reiner.anwander@uni-tuebingen.de

Table of Contents

NMR Spectra

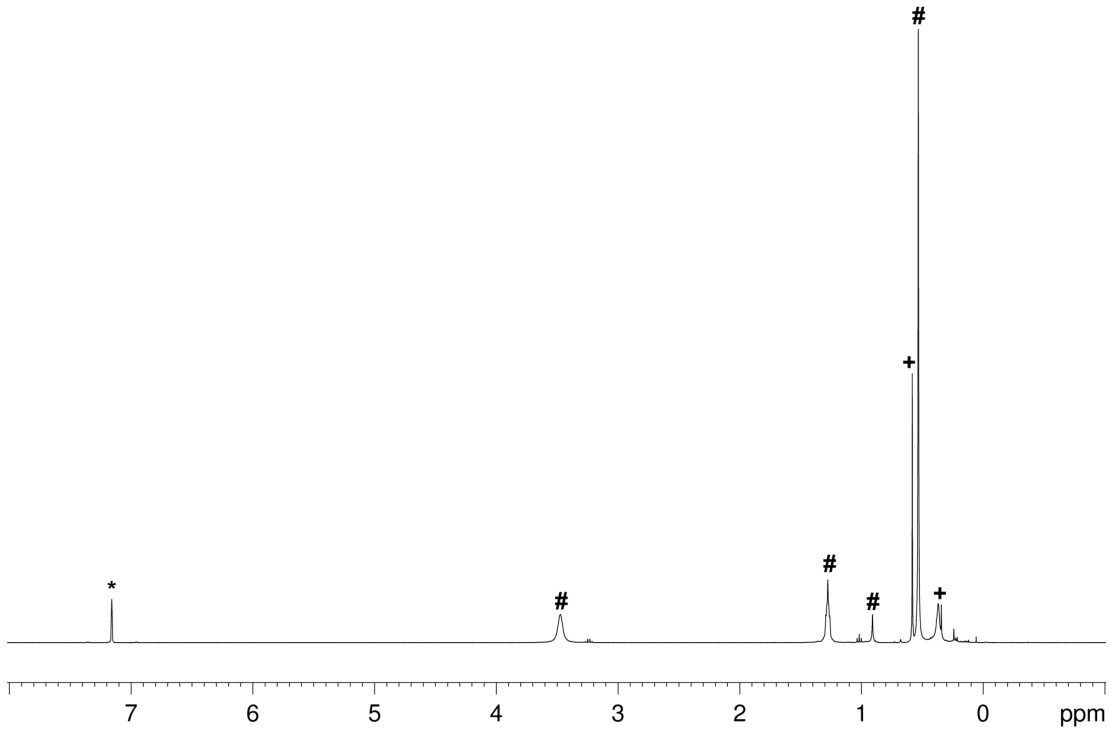

Figure S1. ^{1}H NMR spectrum (400 MHz) of the reaction of $ScCl_3(thf)_3$ with 3 equiv. of $Li[CH(SiMe_3)_2]$ in C_6D_6 at 26 °C. # for **1**. + for complex **2-Sc** as the side product of the reaction. The solvent residual signal is marked with an asterisk.

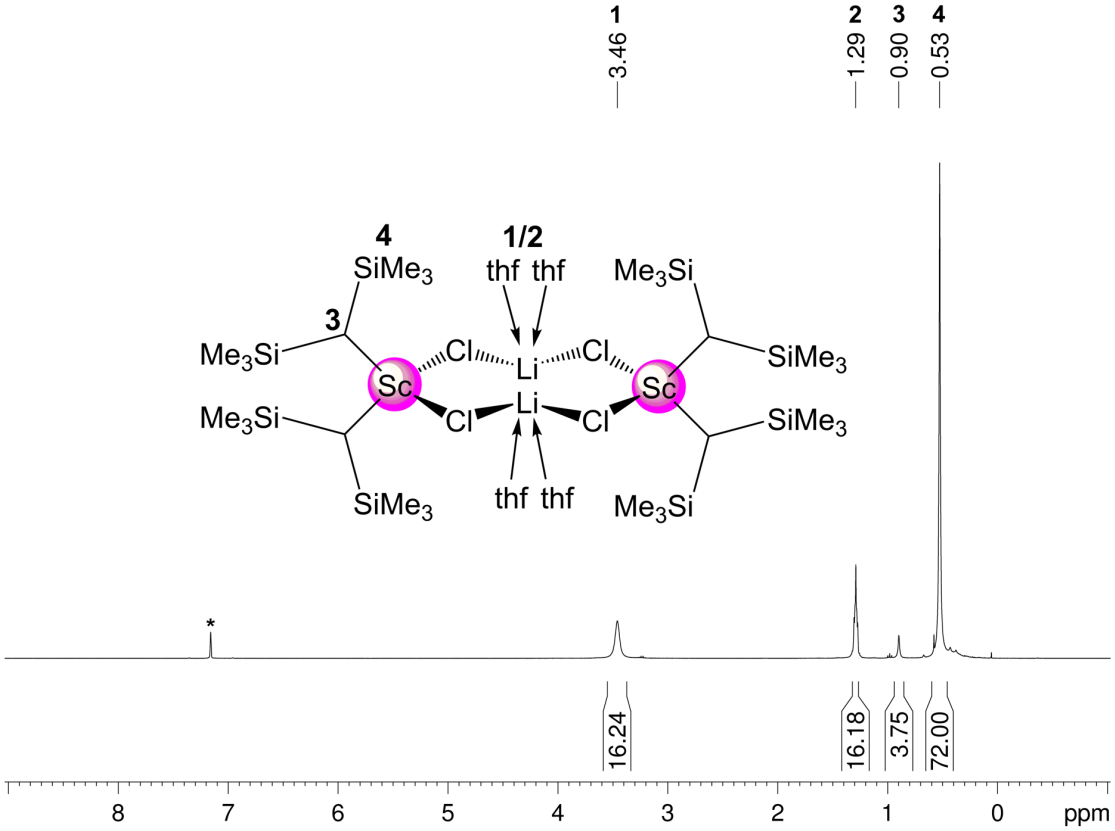

Figure S2. ^{1}H NMR spectrum (400 MHz) of $[Sc\{CH(SiMe_3)_2\}_2(\mu\text{-}Cl)_2Li(thf)_2]_2$ (**1**) in C_6D_6 at 26 °C. The solvent residual signal is marked with an asterisk.

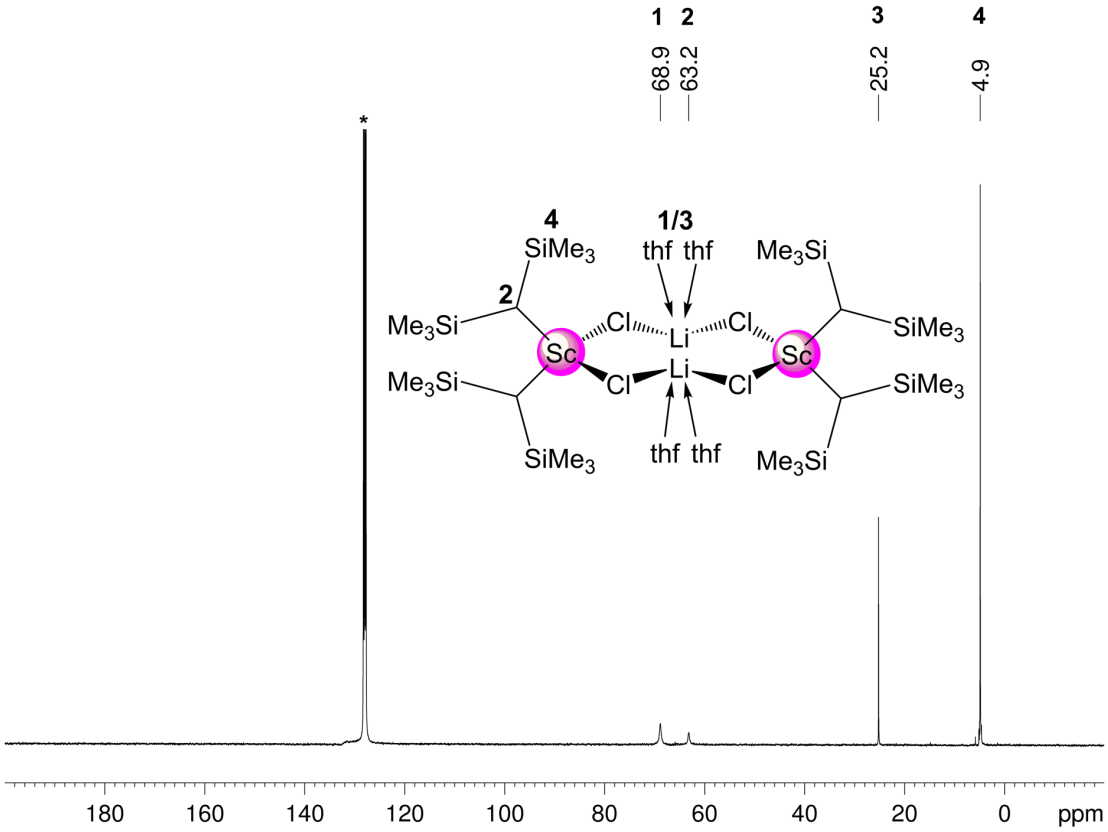

Figure S3. $^{13}C\{^{1}H\}$ NMR spectrum (101 MHz) of $[Sc\{CH(SiMe_3)_2\}_2(\mu\text{-}Cl)_2Li(thf)_2]_2$ (**1**) in C_6D_6 at 26 °C. The solvent residual signal is marked with an asterisk.

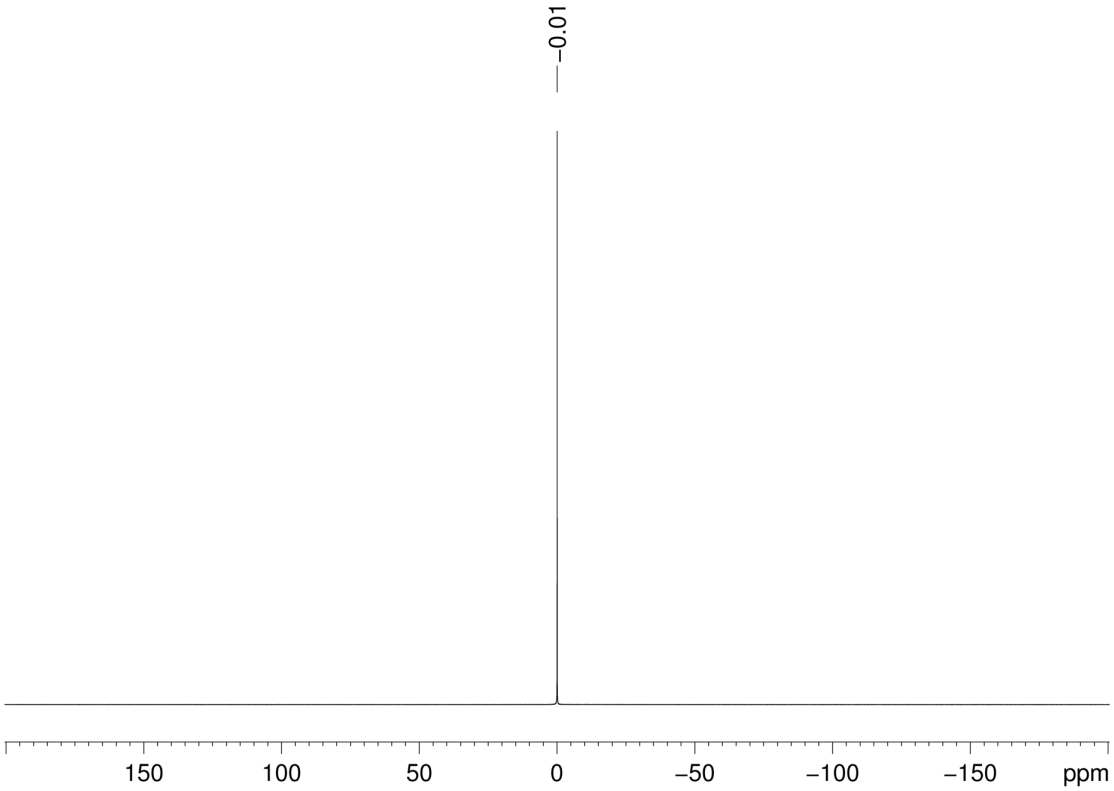

Figure S4. ^{7}Li NMR spectrum (97 MHz) of $[Sc\{CH(SiMe_3)_2\}_2(\mu\text{-}Cl)_2Li(thf)_2]_2$ (**1**) in C_6D_6 at 26 °C.

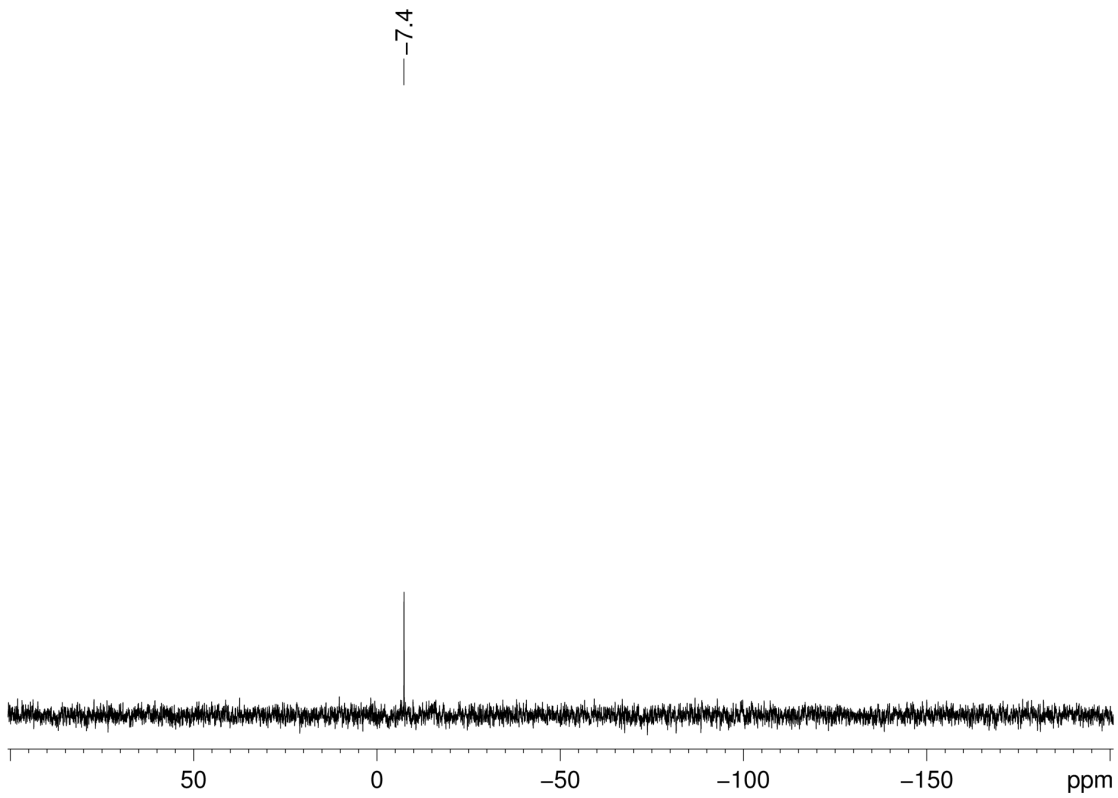

Figure S5. ^{29}Si INEPT NMR spectrum (50 MHz) of $[Sc\{CH(SiMe_3)_2\}_2(\mu\text{-}Cl)_2Li(thf)_2]_2$ (**1**) in C_6D_6 at 26 °C.

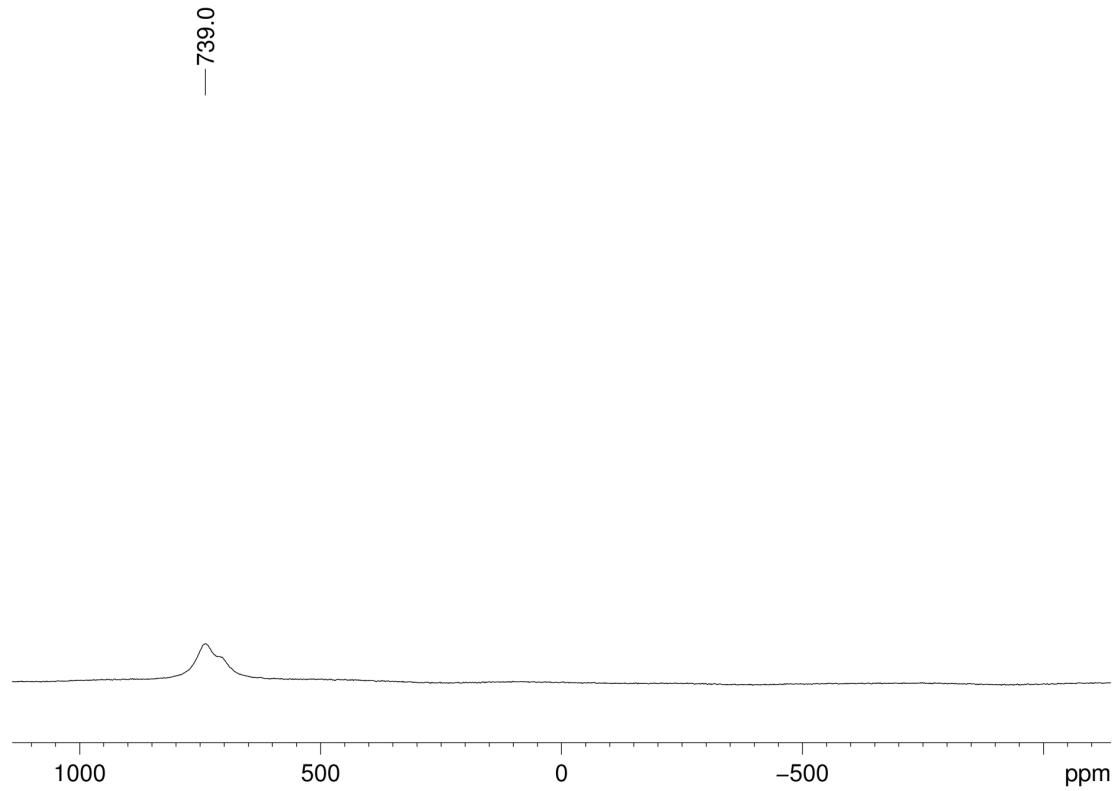

Figure S6. ^{45}Sc NMR spectrum (122 MHz) of $[Sc\{CH(SiMe_3)_2\}_2(\mu\text{-}Cl)_2Li(thf)_2]_2$ (**1**) in C_6D_6 at 26 °C. The shape of the signal is attributed to partial loss of donor solvent (cf. Figure S7).

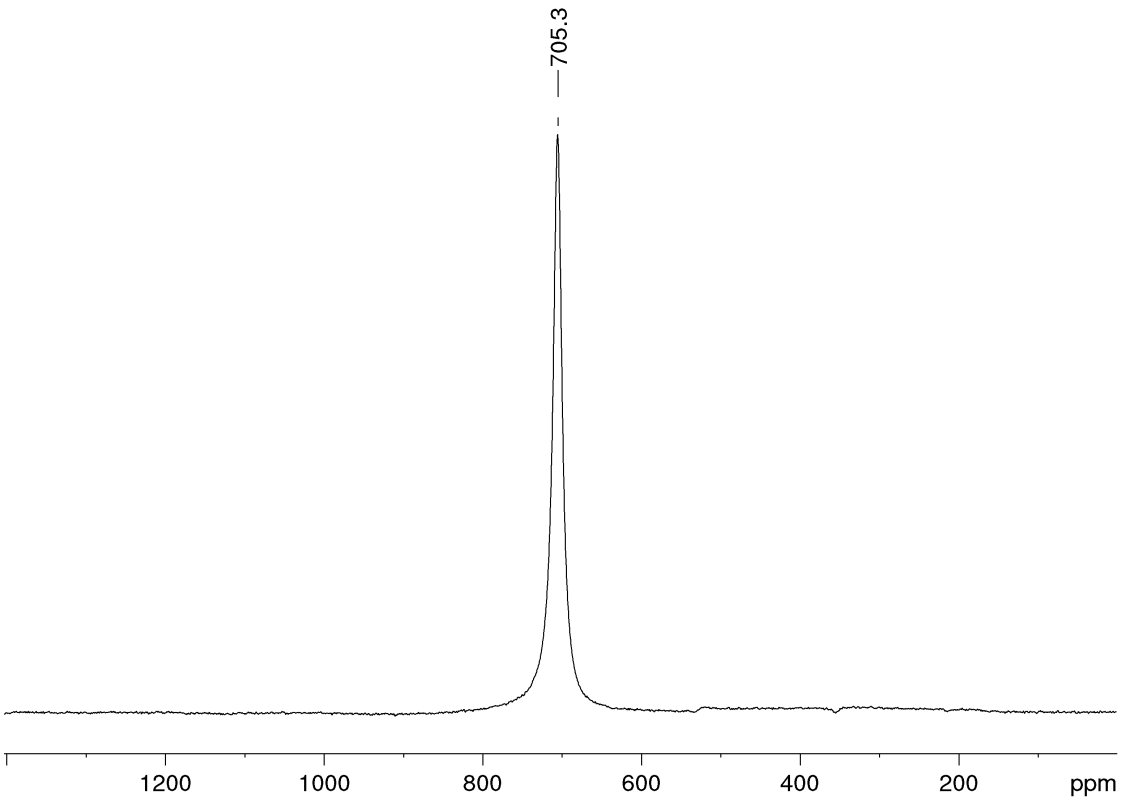

Figure S7. ^{45}Sc NMR spectrum (122 MHz) of [Sc{CH(SiMe$_3$)$_2$}$_2$(μ-Cl)$_2$Li(thf)$_2$]$_2$ (**1**) in [D$_8$]THF at 26 °C.

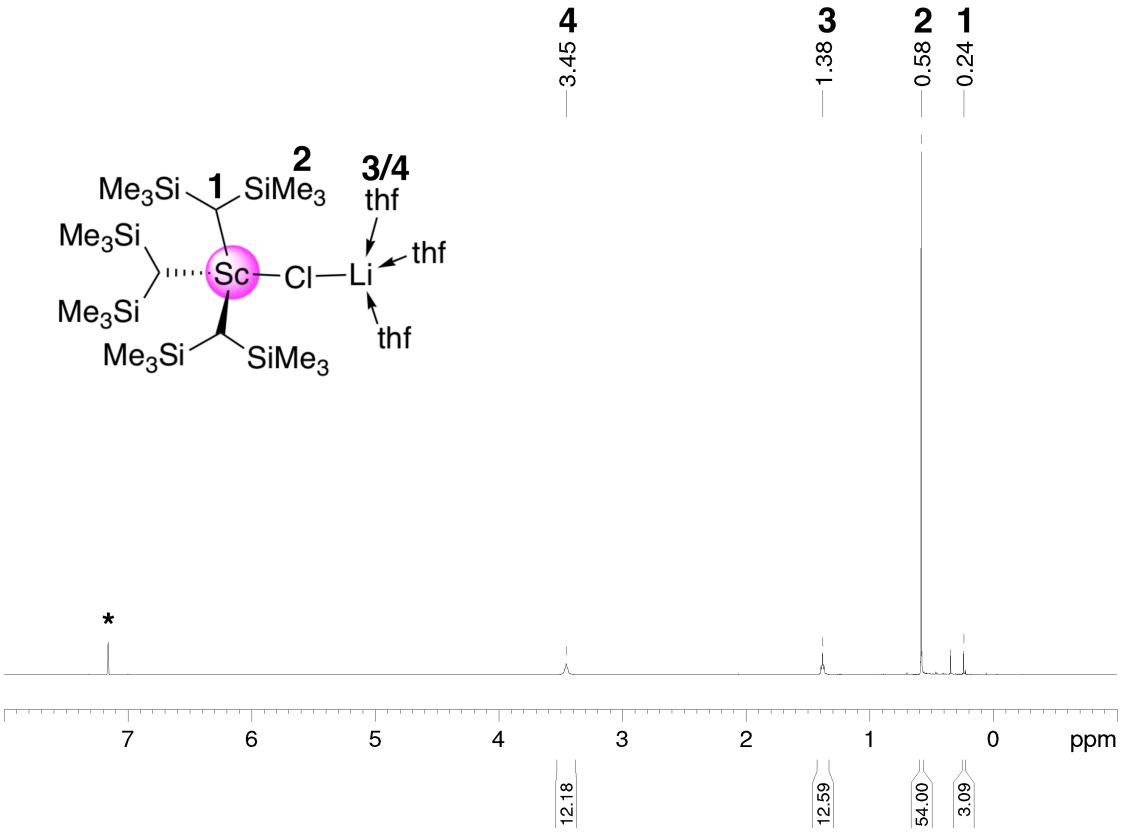

Figure S8. ^{1}H NMR spectrum (500 MHz) of Sc[CH(SiMe$_3$)$_2$]$_3$(μ-Cl)Li(thf)$_3$ (**2-Sc**) in C$_6$D$_6$ at 26 °C. The solvent residual signal is marked with an asterisk.

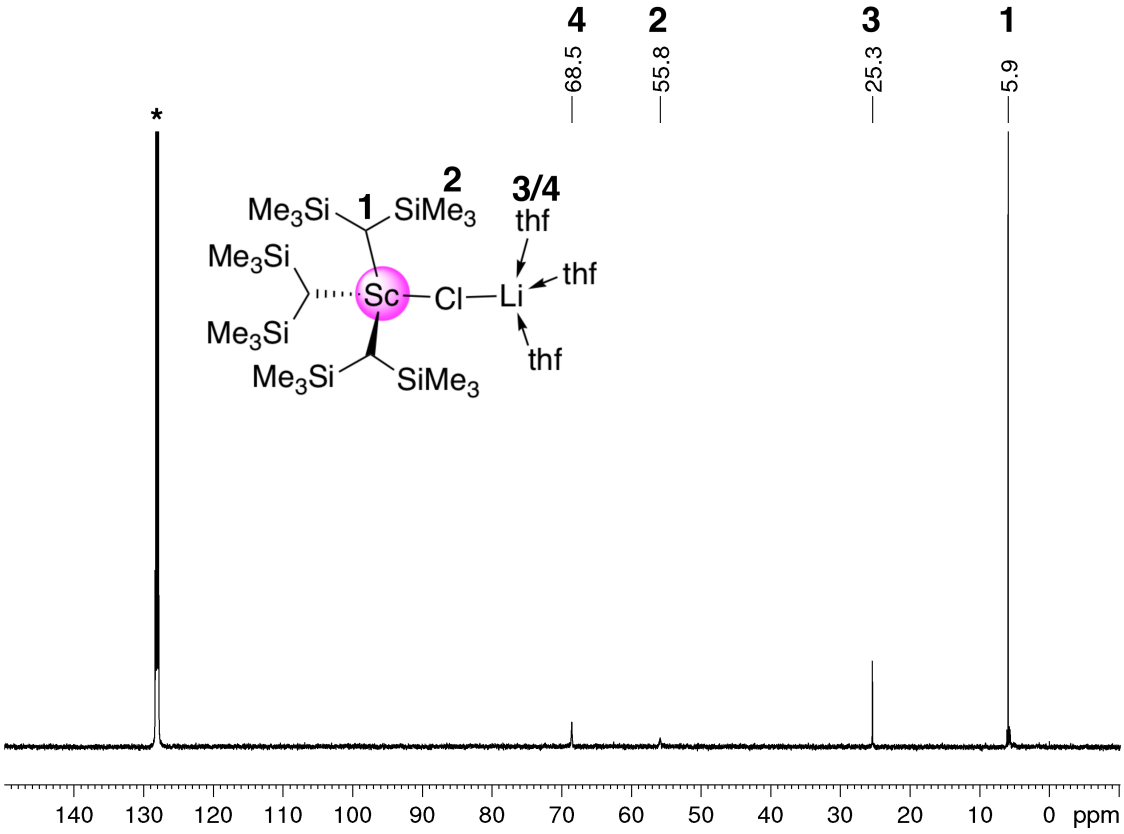

Figure S9. $^{13}C\{^{1}H\}$ NMR spectrum (126 MHz) of $Sc[CH(SiMe_3)_2]_3(\mu\text{-}Cl)Li(thf)_3$ (**2-Sc**) in C_6D_6 at 26 °C. The solvent residual signal is marked with an asterisk.

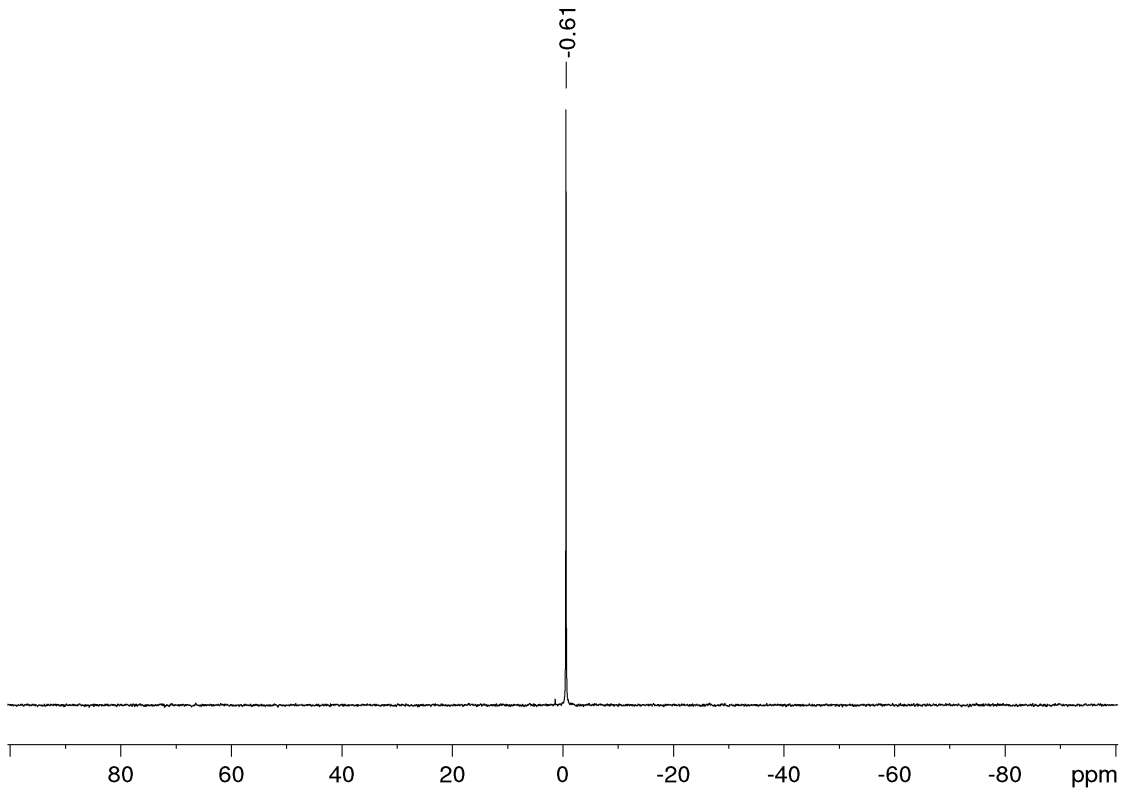

Figure S10. $^{7}Li\{^{1}H\}$ NMR spectrum (194 MHz) of $Sc[CH(SiMe_3)_2]_3(\mu\text{-}Cl)Li(thf)_3$ (**2-Sc**) in C_6D_6 at 26 °C.

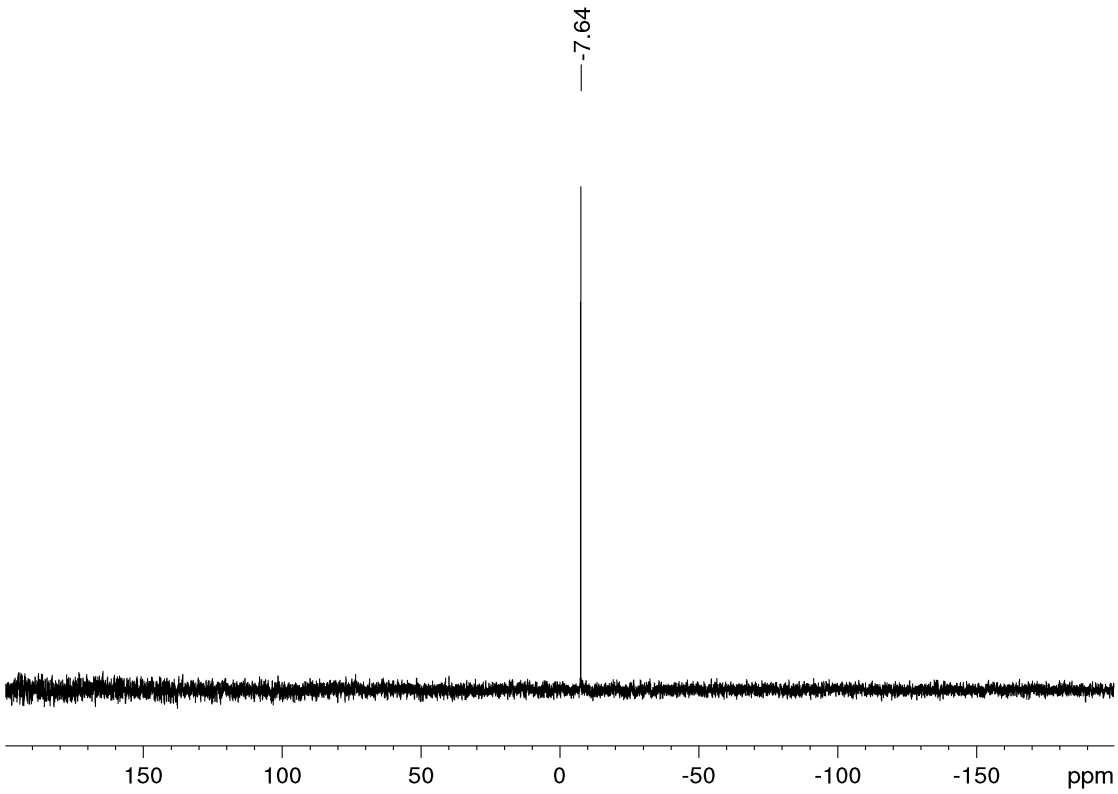

Figure S11. ^{29}Si INEPT NMR spectrum (99 MHz) of Sc[CH(SiMe$_3$)$_2$]$_3$(μ-Cl)Li(thf)$_3$ (**2-Sc**) in C_6D_6 at 26 °C.

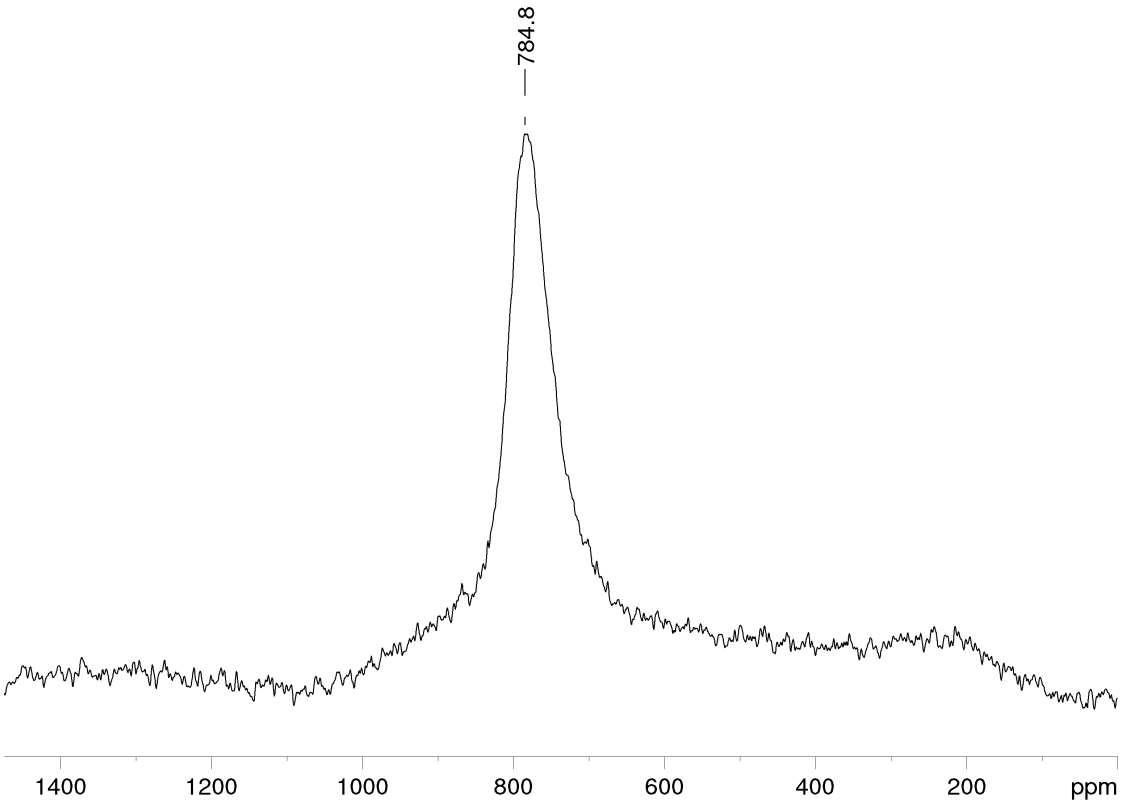

Figure S12. ^{45}Sc NMR spectrum (122 MHz) of [Sc[CH(SiMe$_3$)$_2$]$_3$(μ-Cl)Li(thf)$_3$ (**2-Sc**) in C_6D_6 at 26 °C.

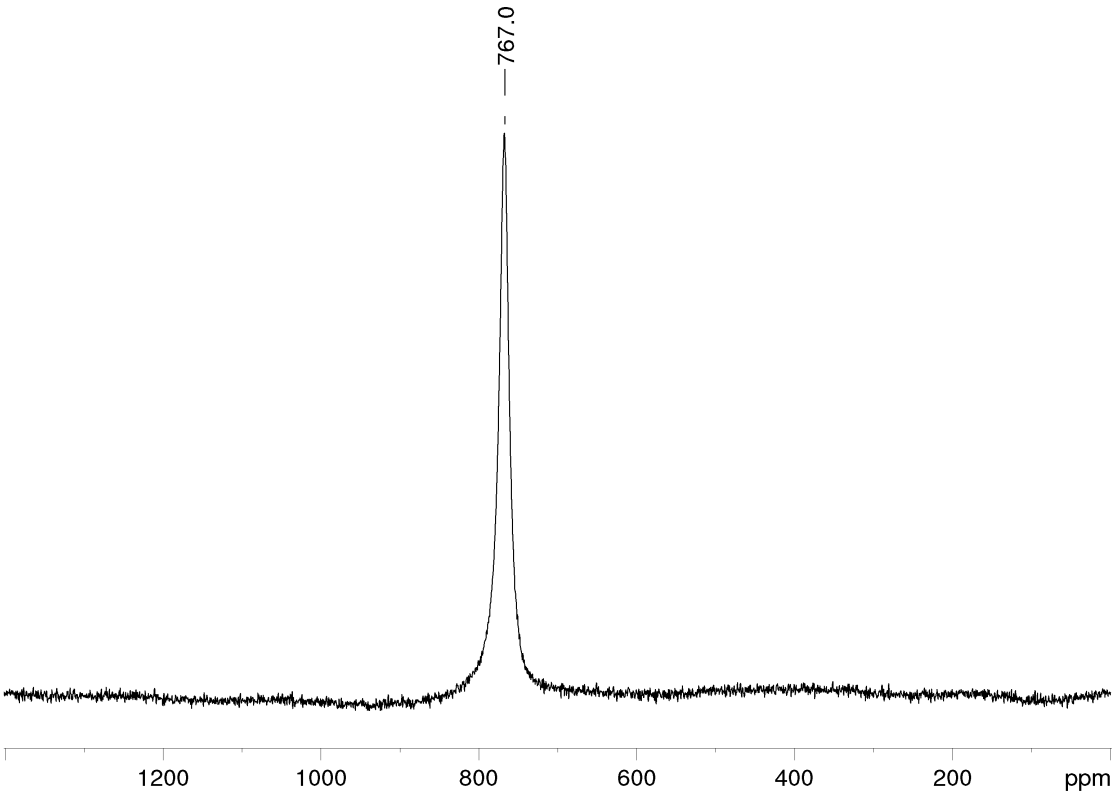

Figure S13. ^{45}Sc NMR spectrum (122 MHz) of [Sc[CH(SiMe$_3$)$_2$]$_3$(μ-Cl)Li(thf)$_3$ (**2-Sc**) in [D$_8$]THF at 26 °C.

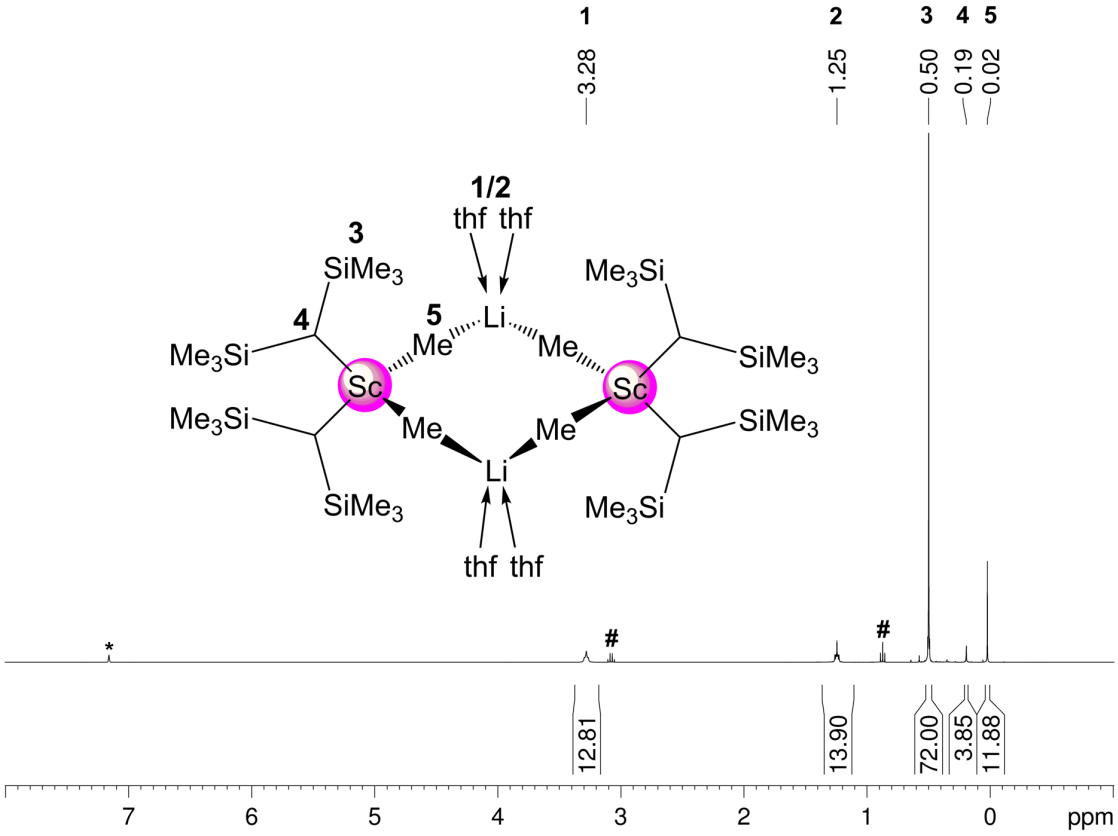

Figure S14. ^{1}H NMR spectrum (500 MHz) of [Sc{CH(SiMe$_3$)$_2$}$_2$(μ-Me)$_2$Li(thf)$_2$]$_2$ (**3**) in C$_6$D$_6$ at 26 °C. The solvent residual signal is marked with an asterisk. # for residual Et$_2$O.

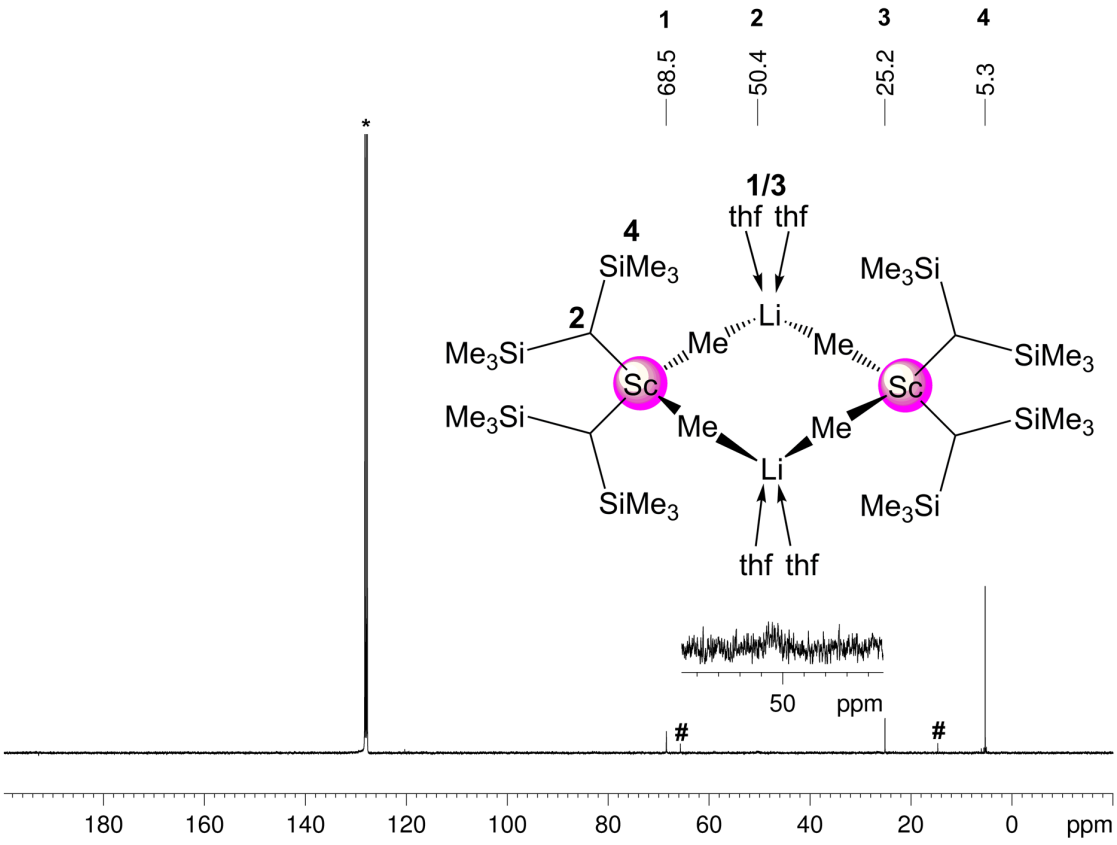

Figure S15. $^{13}C\{^{1}H\}$ NMR spectrum (101 MHz) of $[Sc\{CH(SiMe_3)_2\}_2(\mu\text{-}Me)_2Li(thf)_2]_2$ (**3**) in C_6D_6 at 26 °C. The solvent residual signal is marked with an asterisk. # for residual Et_2O.

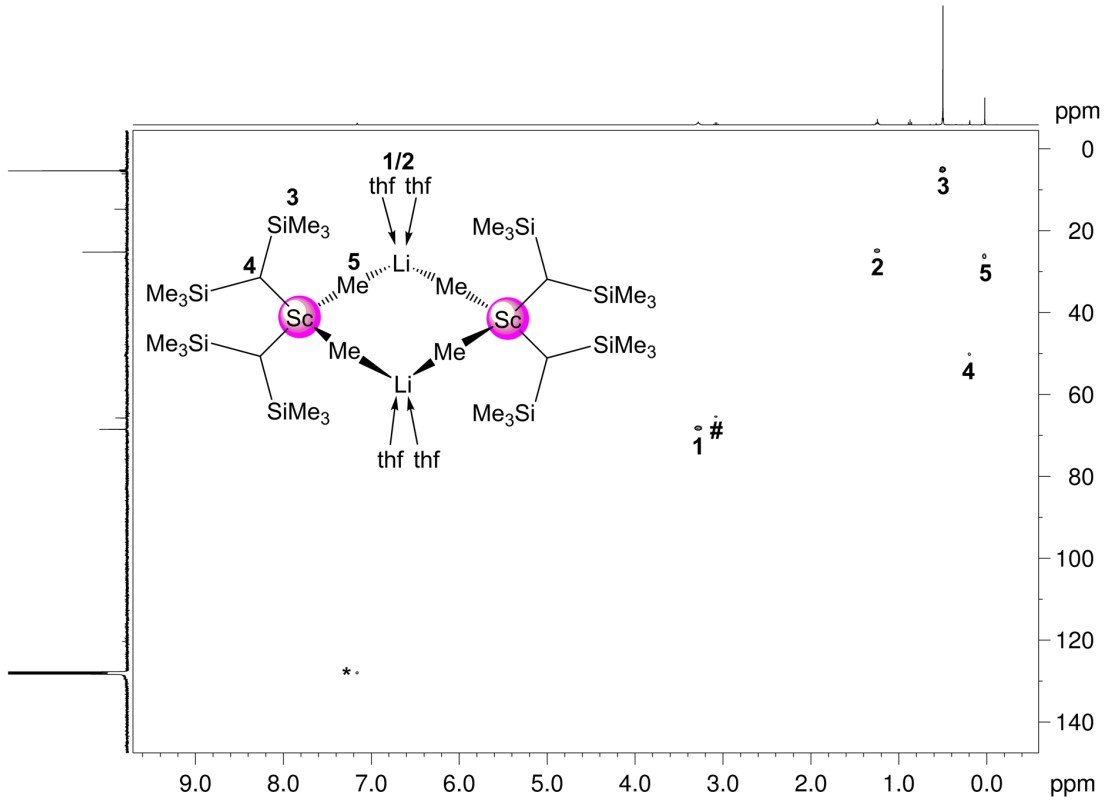

Figure S16. $^{1}H\text{-}^{13}C$ HSQC NMR spectrum of $[Sc\{CH(SiMe_3)_2\}_2(\mu\text{-}Me)_2Li(thf)_2]_2$ (**3**) in C_6D_6 at 26 °C. The solvent residual signal is marked with an asterisk. # for residual Et_2O.

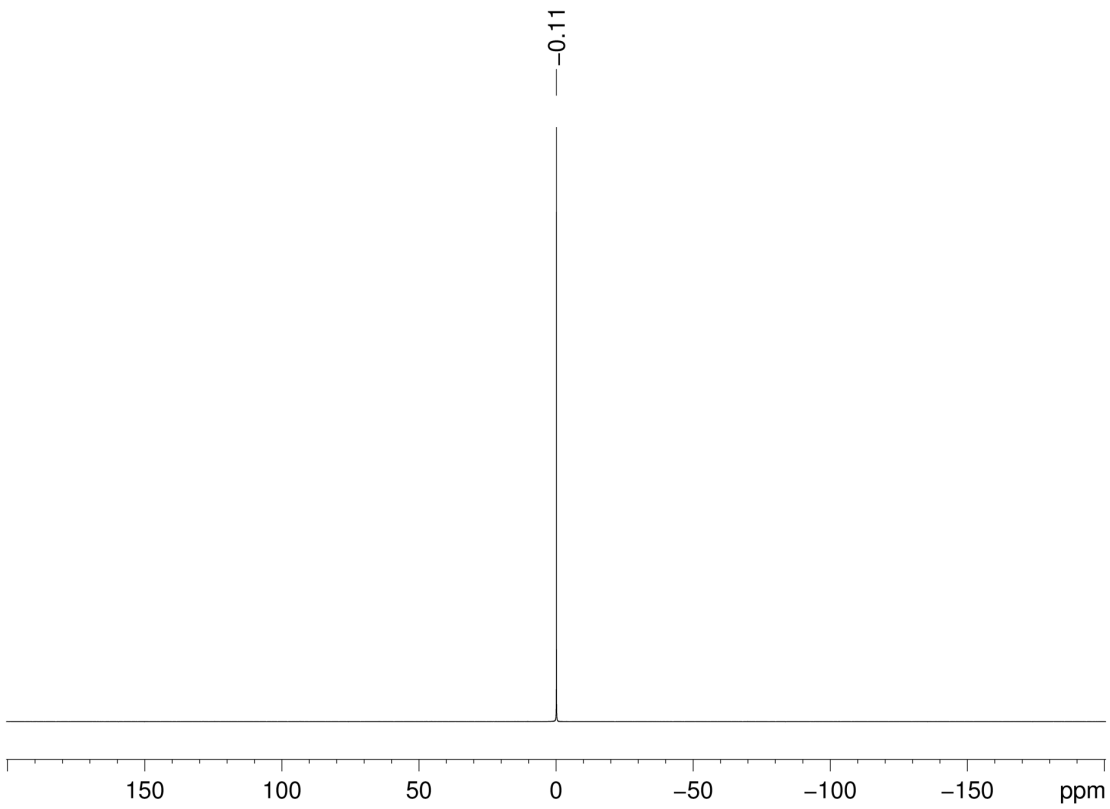

Figure S17. ^{7}Li NMR spectrum (97 MHz) of [Sc{CH(SiMe$_3$)$_2$}$_2$(μ-Me)$_2$Li(thf)$_2$]$_2$ (**3**) in C_6D_6 at 26 °C.

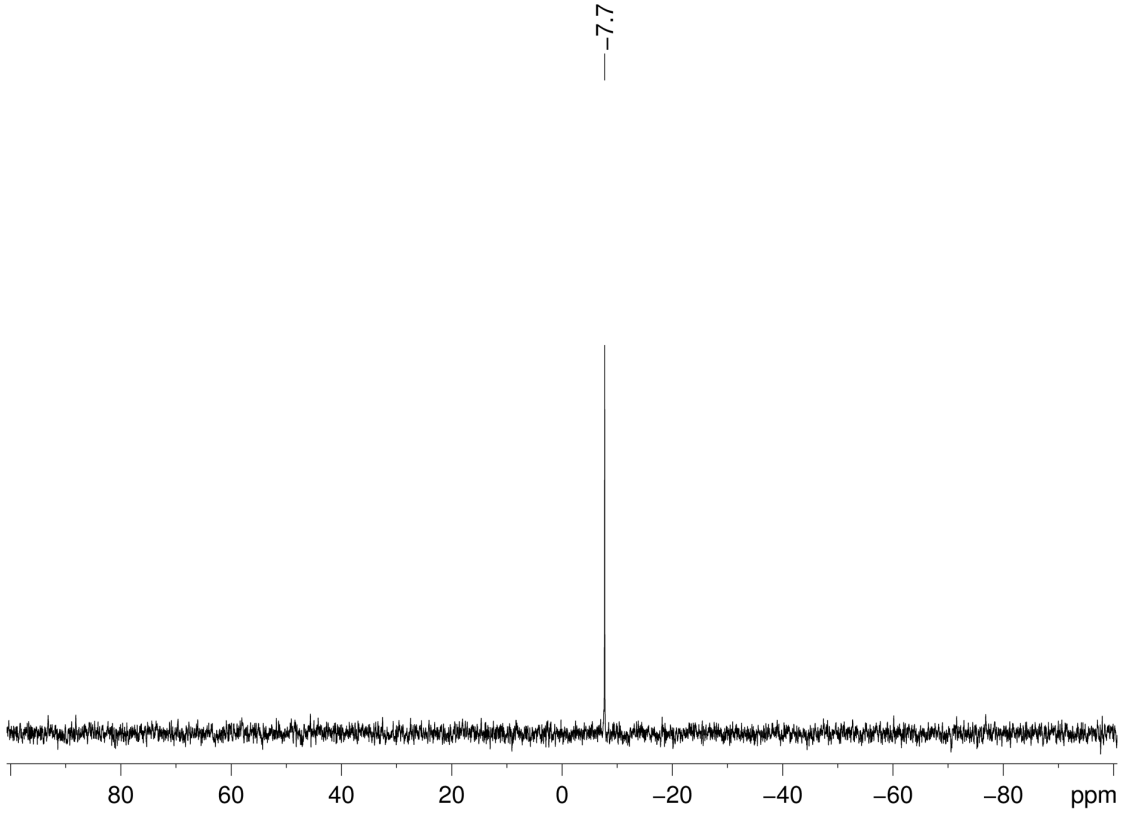

Figure S18. ^{29}Si INEPT NMR spectrum (50 MHz) of [Sc{CH(SiMe$_3$)$_2$}$_2$(μ-Me)$_2$Li(thf)$_2$]$_2$ (**3**) in C_6D_6 at 26 °C.

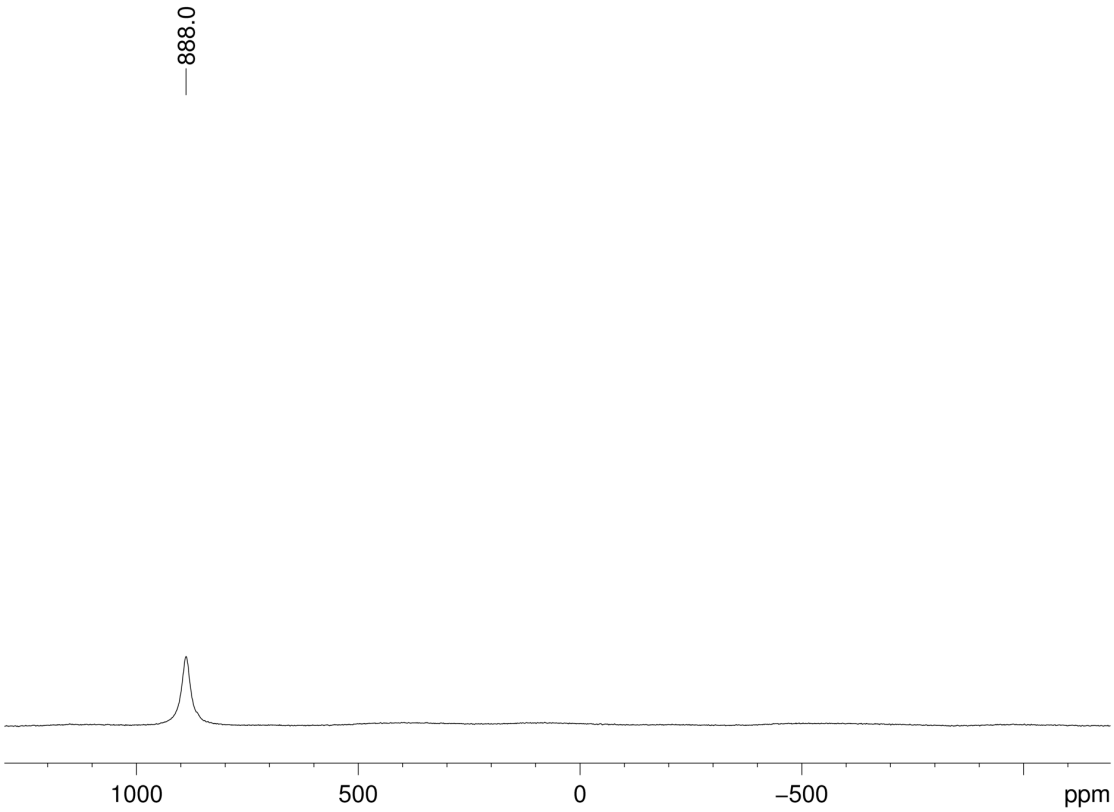

Figure S19. ^{45}Sc NMR spectrum (122 MHz) of $[Sc\{CH(SiMe_3)_2\}_2(\mu\text{-}Me)_2Li(thf)_2]_2$ (**3**) in C_6D_6 at 26 °C.

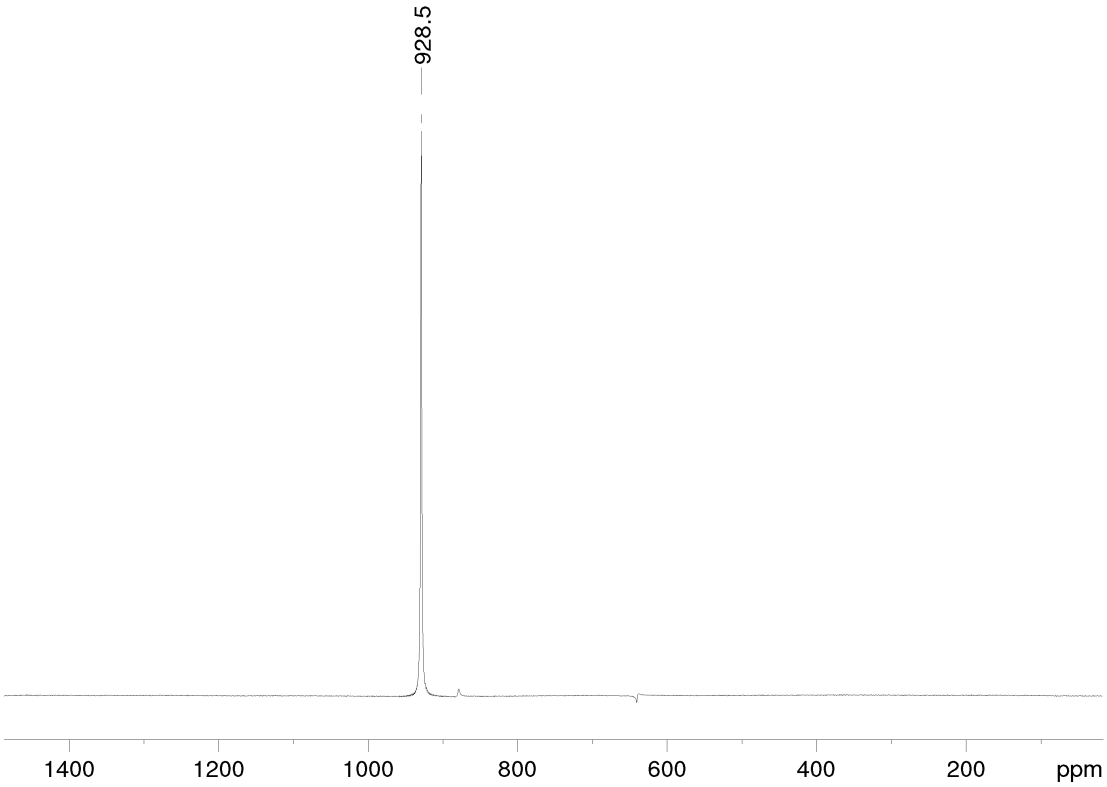

Figure S20. ^{45}Sc NMR spectrum (122 MHz) of $[Sc\{CH(SiMe_3)_2\}_2(\mu\text{-}Me)_2Li(thf)_2]_2$ (**3**) in $[D_8]$THF at 26 °C.

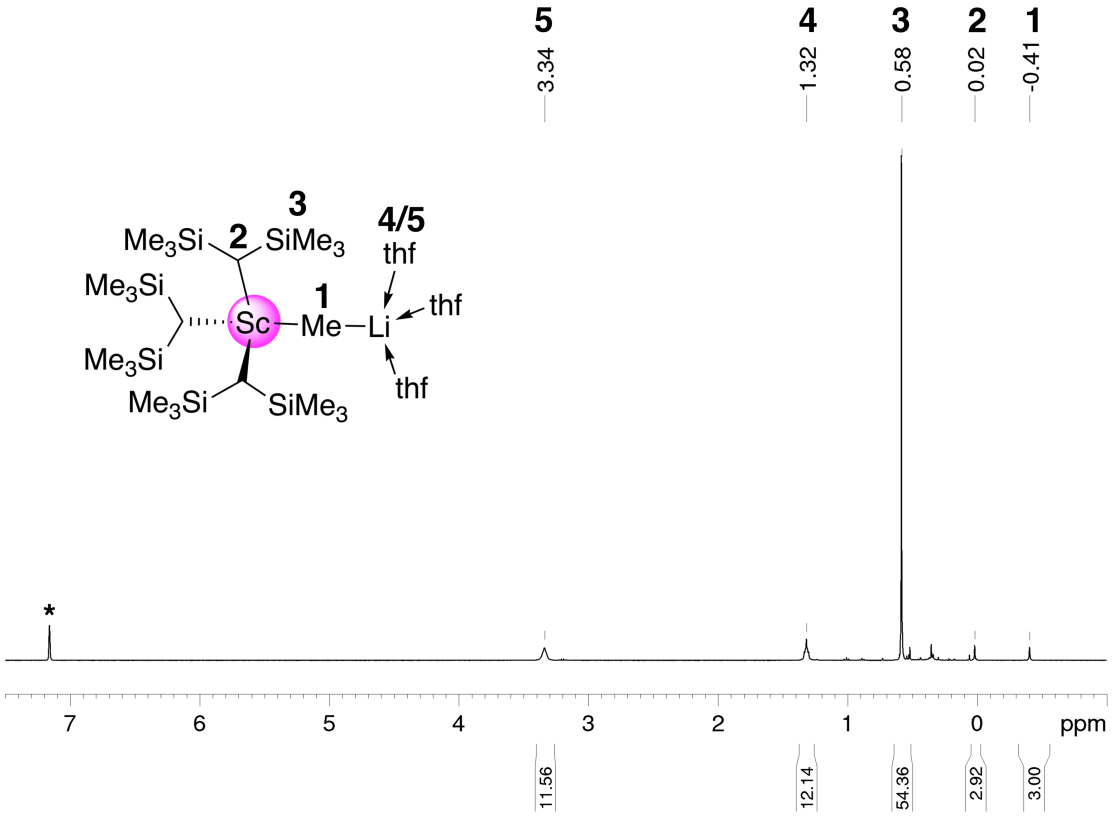

Figure S21. ^{1}H NMR spectrum (400 MHz) of Sc[CH(SiMe$_3$)$_2$]$_3$(μ-Me)Li(thf)$_3$ (**4**) in C_6D_6 at 26 °C. The solvent residual signal is marked with an asterisk.

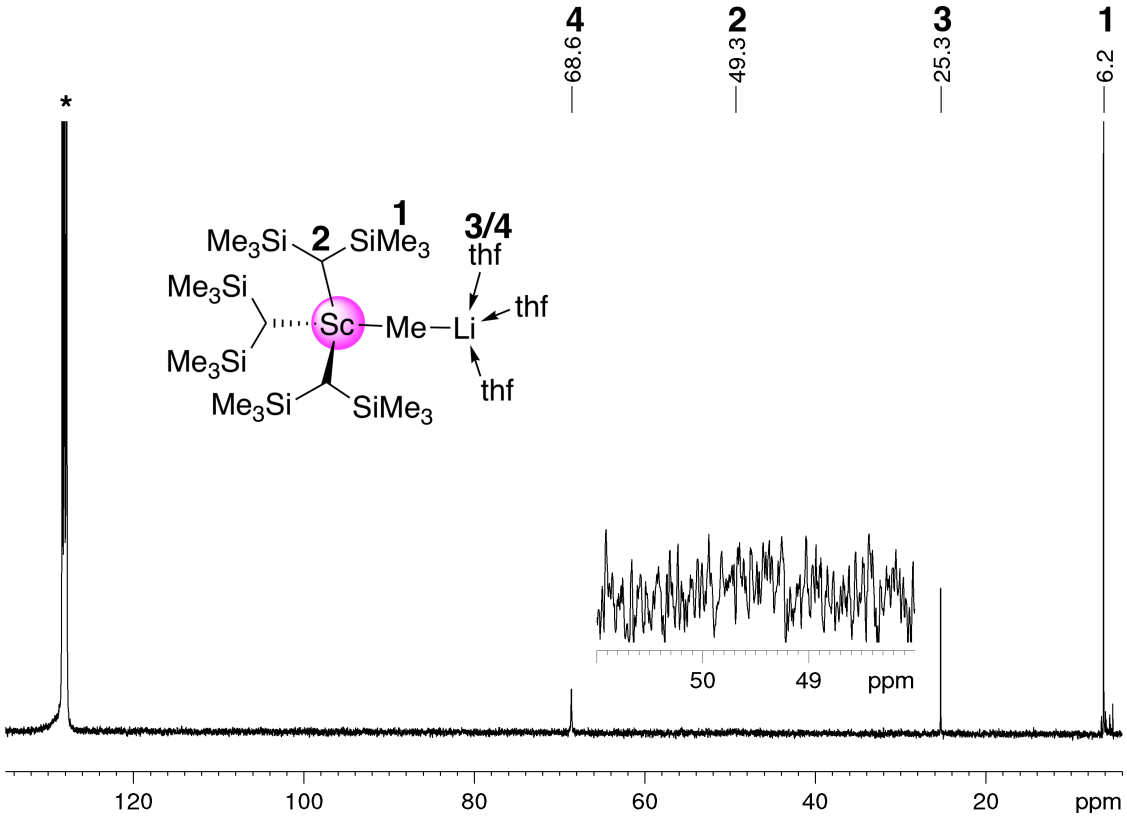

Figure S22. ^{13}C{^{1}H} NMR spectrum (100 MHz) of Sc[CH(SiMe$_3$)$_2$]$_3$(μ-Me)Li(thf)$_3$ (**4**) in C_6D_6 at 26 °C. The solvent residual signal is marked with an asterisk.

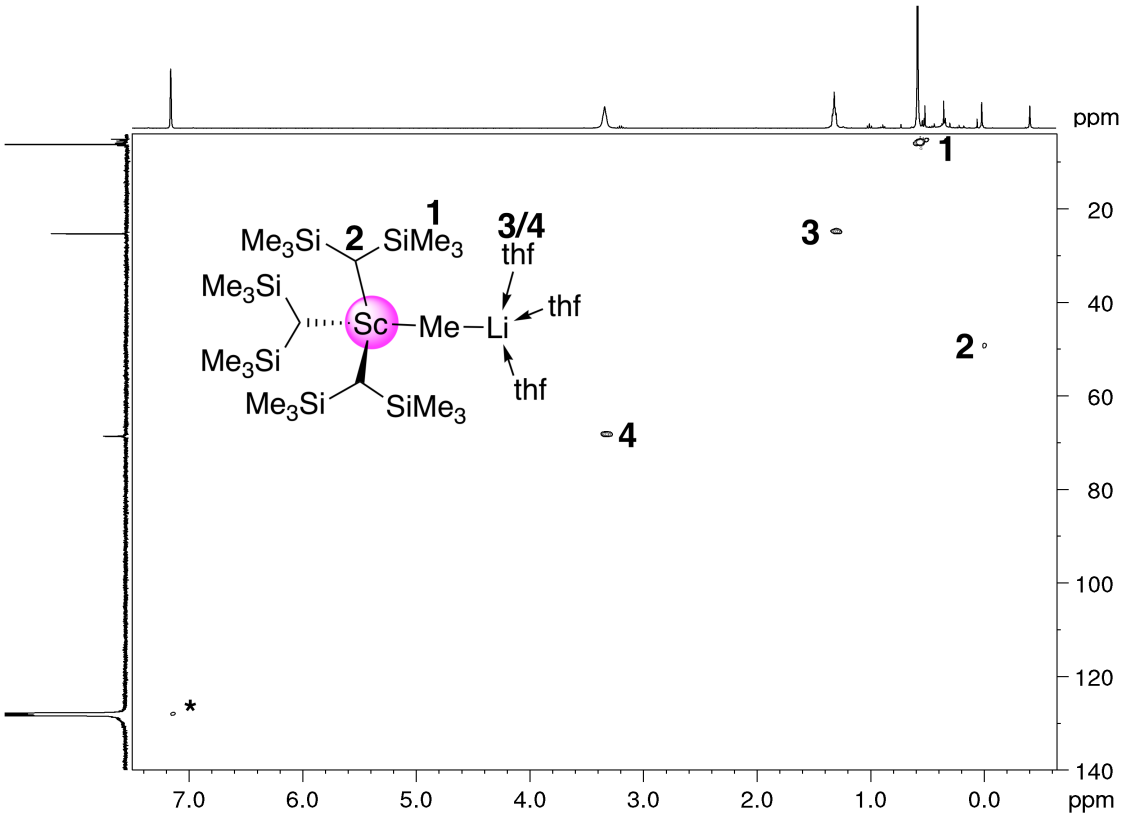

Figure S23. ^{1}H-^{13}C HSQC NMR spectrum of $Sc[CH(SiMe_3)_2]_3(\mu\text{-}Me)Li(thf)_3$ (**4**) in C_6D_6 at 26 °C. The solvent residual signal is marked with an asterisk.

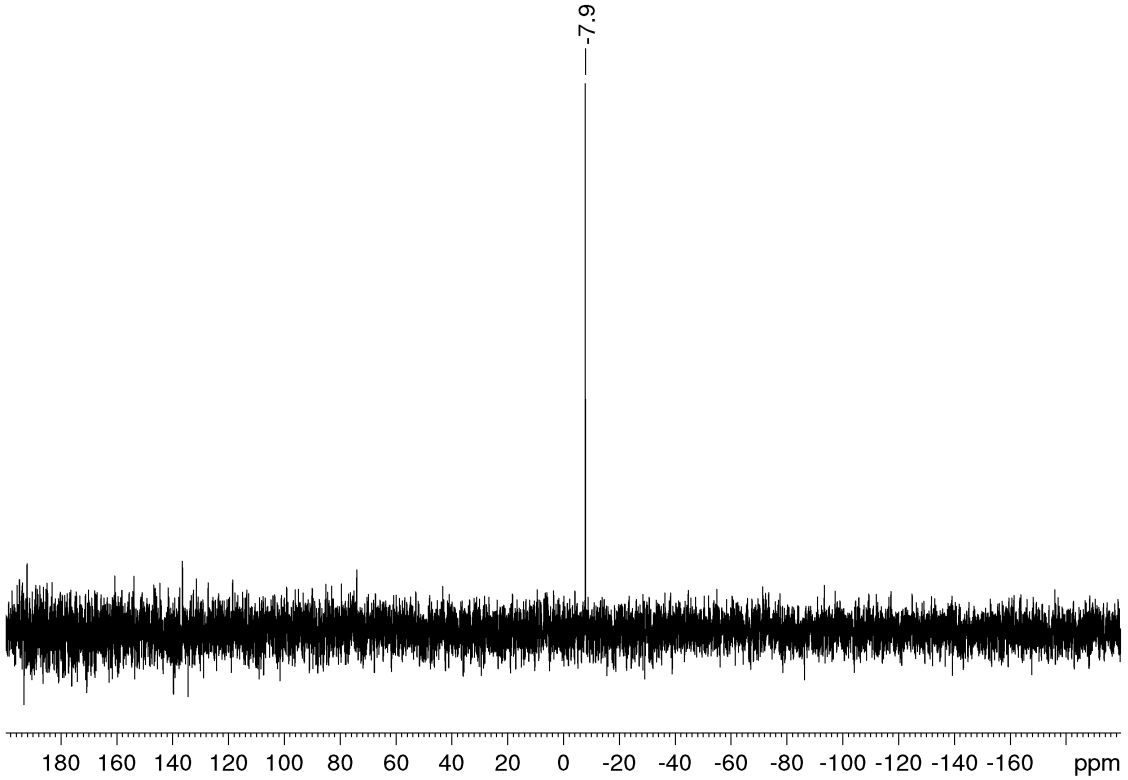

Figure S24. ^{29}Si DEPT45 NMR spectrum (99 MHz) of $Sc[CH(SiMe_3)_2]_3(\mu\text{-}Me)Li(thf)_3$ (**4**) in C_6D_6 at 26 °C.

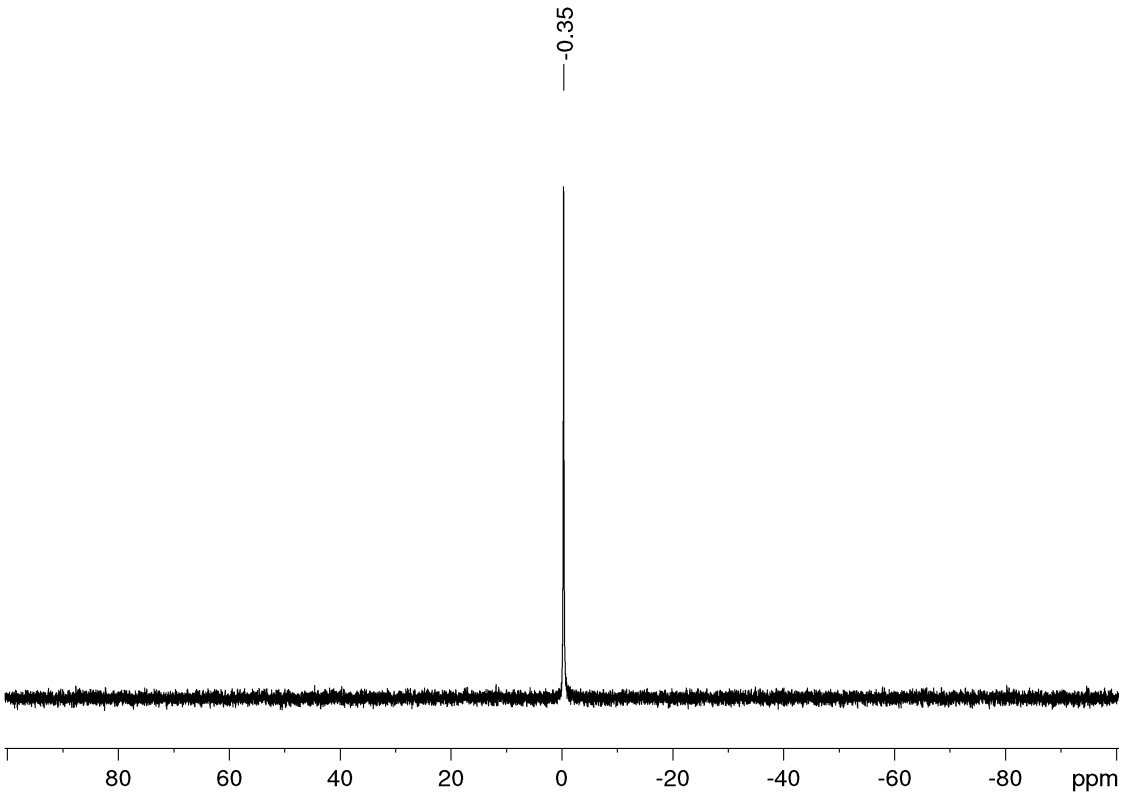

Figure S25. $^{7}Li\{^{1}H\}$ NMR spectrum (194 MHz) of $Sc[CH(SiMe_3)_2]_3(\mu\text{-}Me)Li(thf)_3$ (**4**) in C_6D_6 at 26 °C.

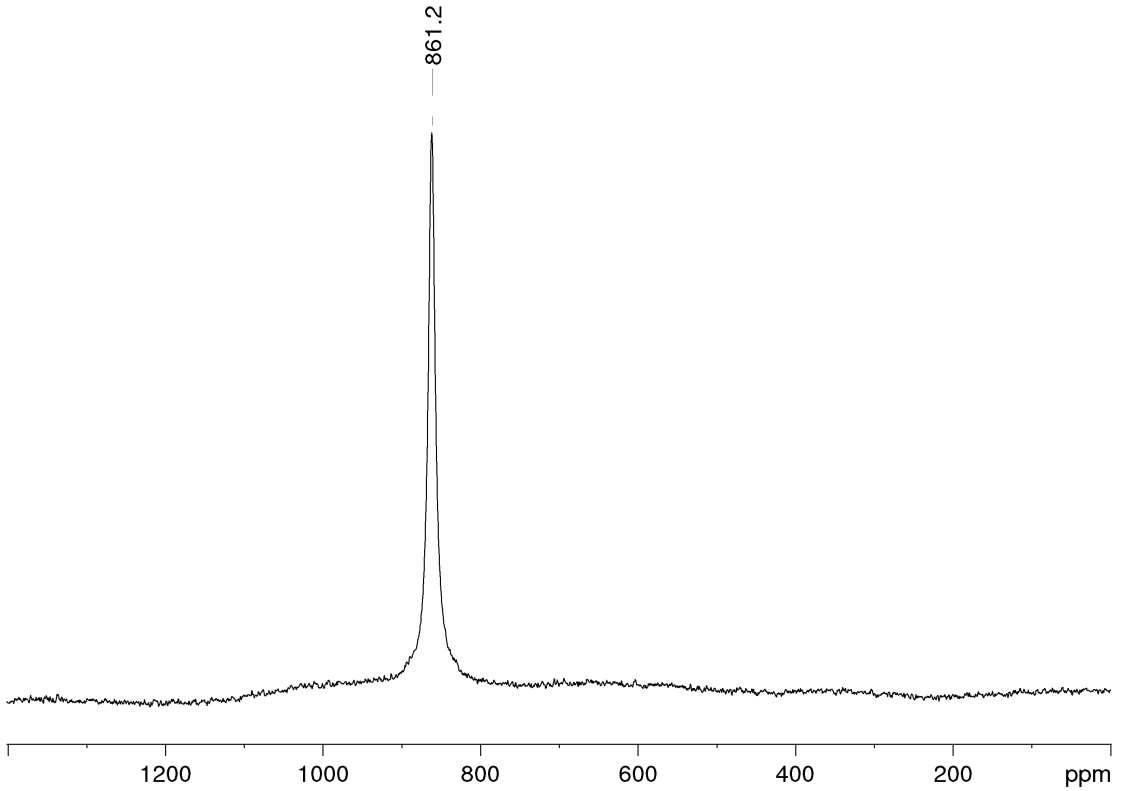

Figure S26. ^{45}Sc NMR spectrum (122 MHz) of $Sc[CH(SiMe_3)_2]_3(\mu\text{-}Me)Li(thf)_3$ (**4**) in C_6D_6 at 26 °C

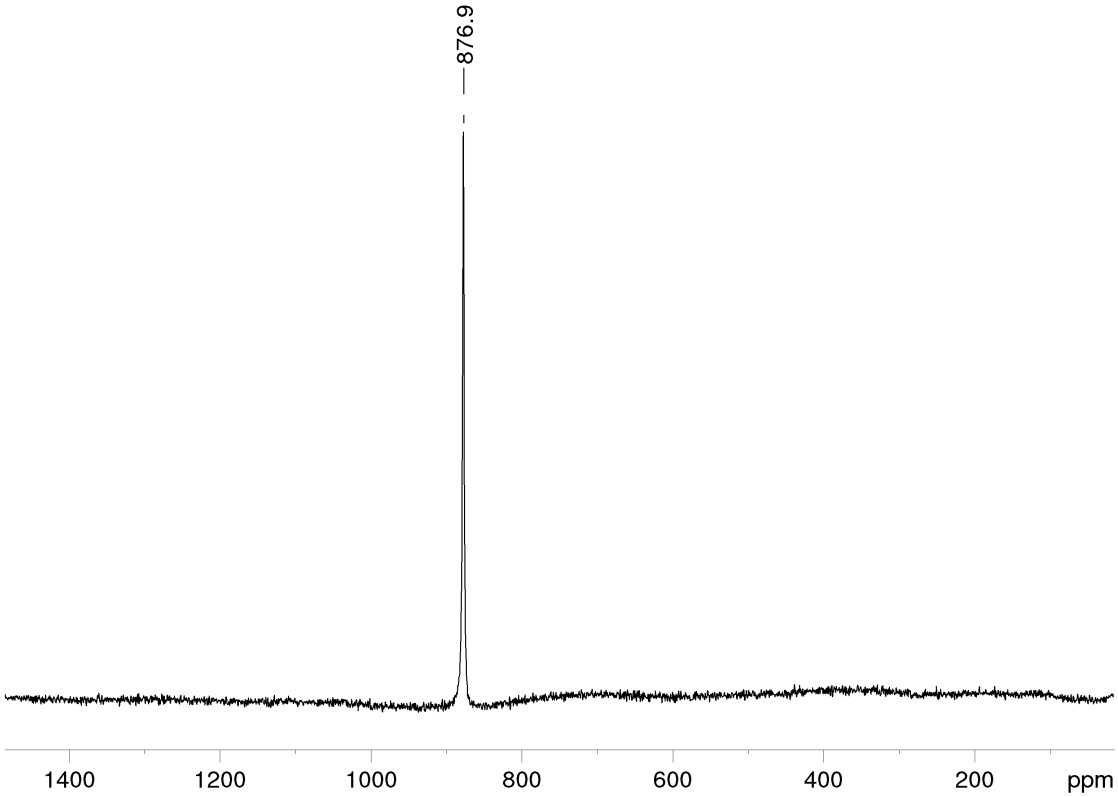

Figure S27. ^{45}Sc NMR spectrum (122 MHz) of [Sc[CH(SiMe$_3$)$_2$]$_3$(μ-Me)Li(thf)$_3$ (**4**) in [D$_8$]THF at 26 °C.

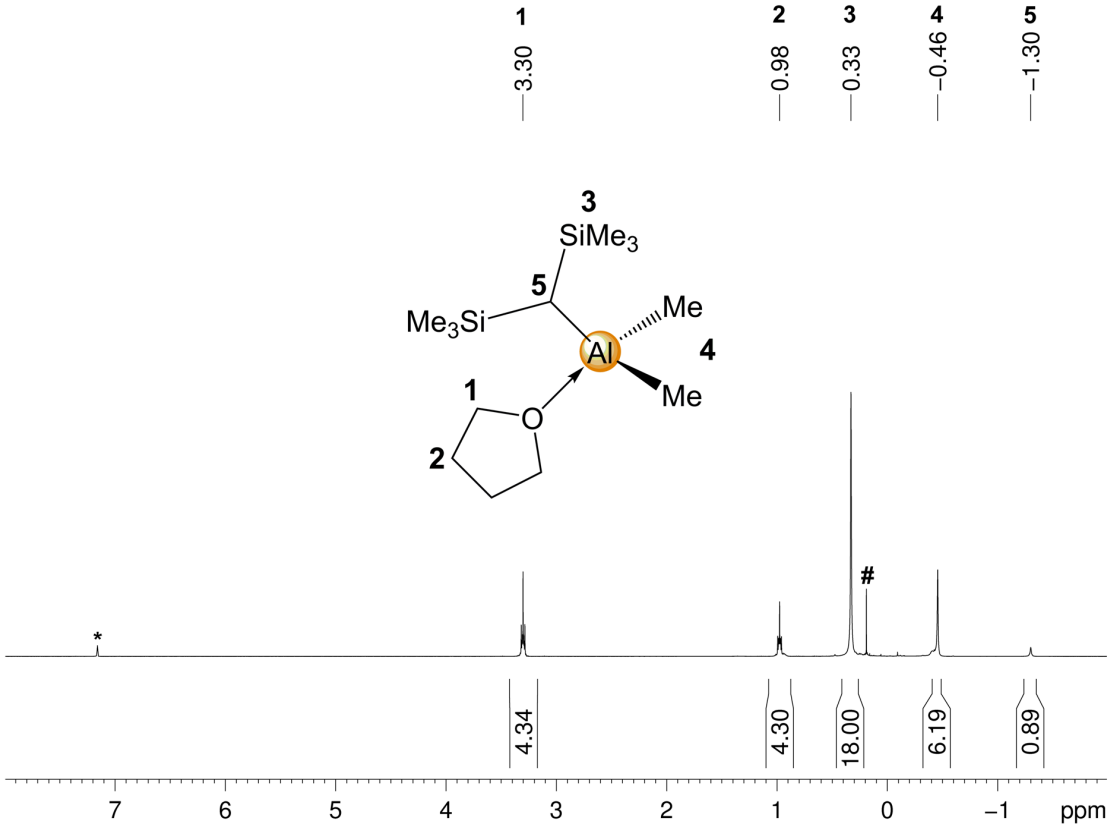

Figure S28. ^{1}H NMR spectrum (400 MHz) of Al[CH(SiMe$_3$)$_2$]Me$_2$(thf) (**5**) in C$_6$D$_6$ at 26 °C. The solvent residual signal is marked with an asterisk. # for unknown by-product.

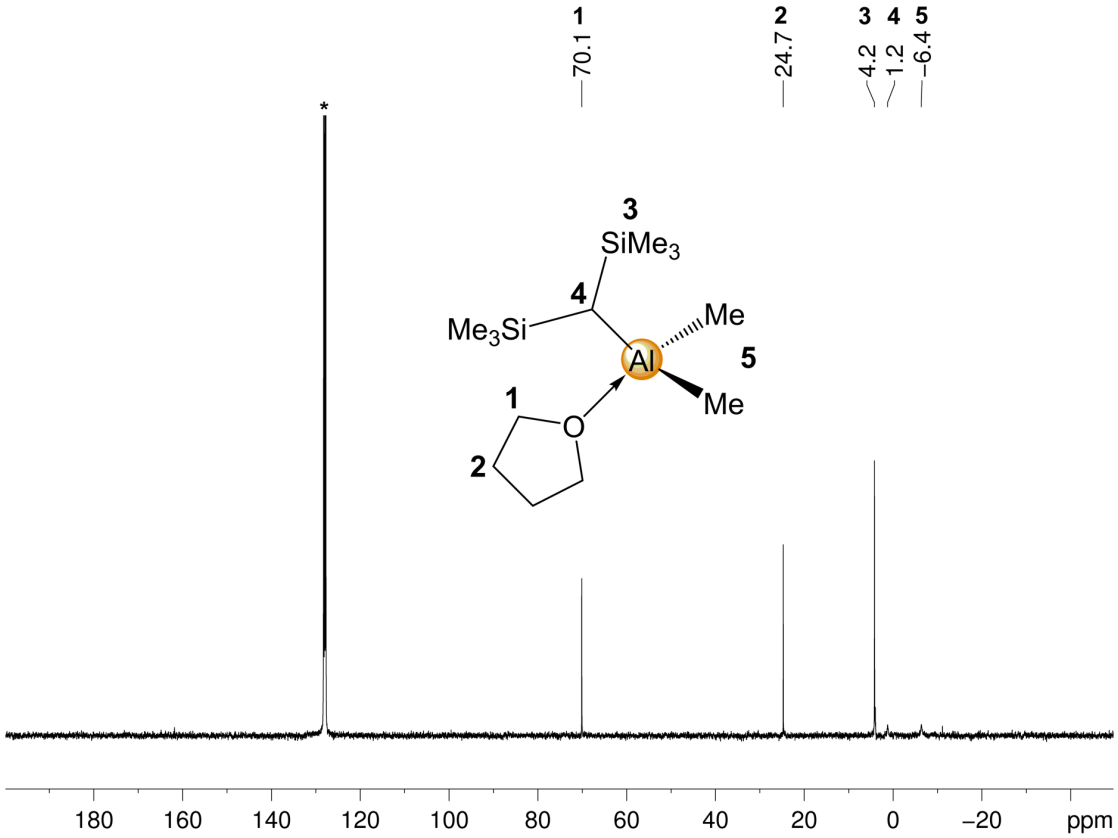

Figure S29. $^{13}C\{^{1}H\}$ NMR spectrum (101 MHz) of $Al[CH(SiMe_3)_2]Me_2(thf)$ (**5**) in C_6D_6 at 26 °C. The solvent residual signal is marked with an asterisk.

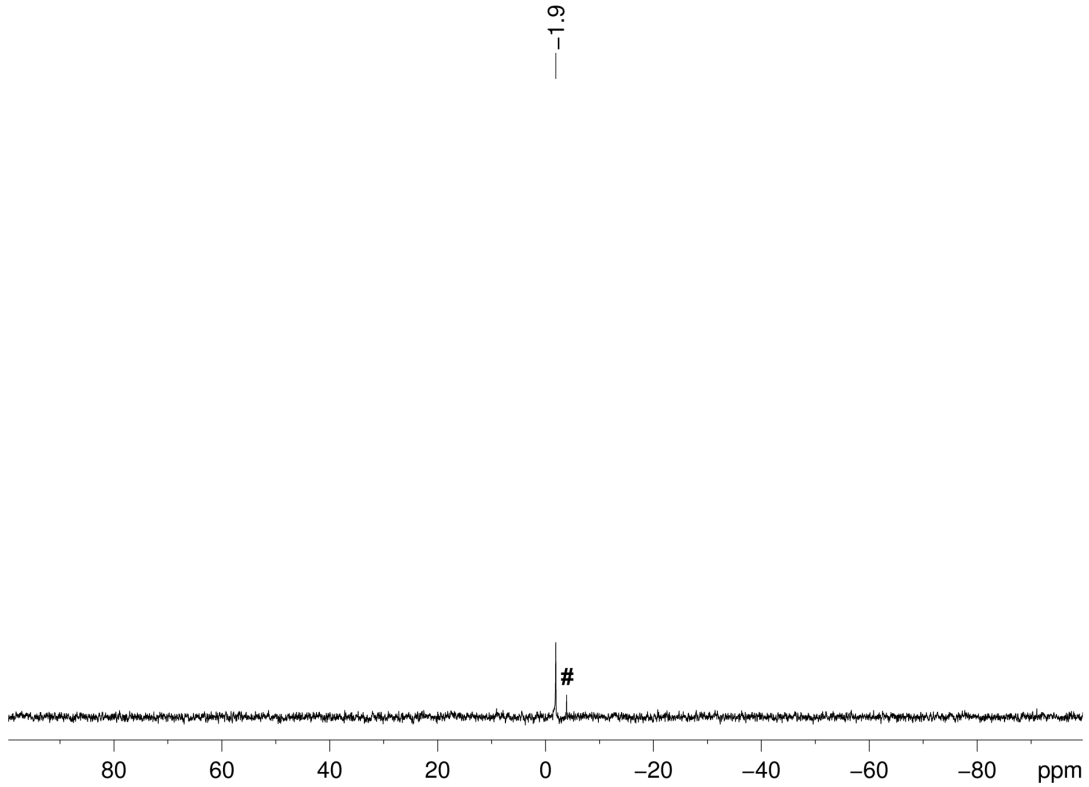

Figure S30. ^{29}Si INEPT NMR spectrum (50 MHz) of $Al[CH(SiMe_3)_2]Me_2(thf)$ (**5**) in C_6D_6 at 26 °C. # for unknown by-product.

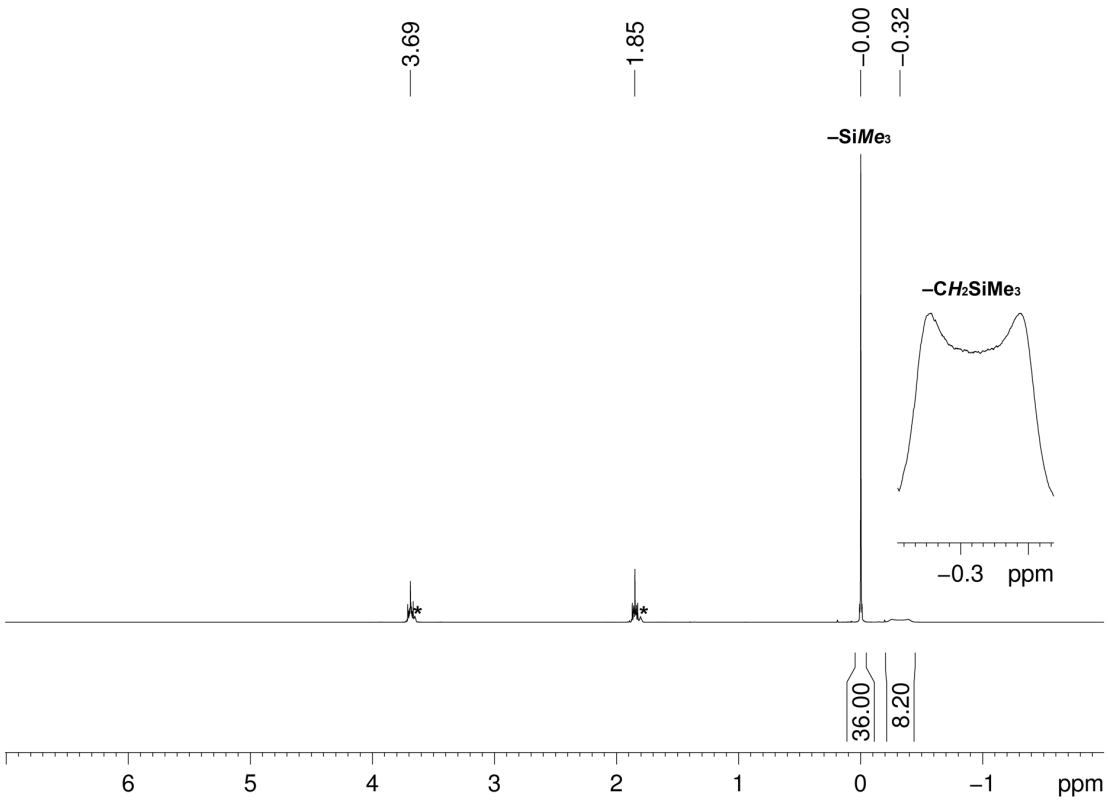

Figure S31. ^{1}H NMR spectrum (500 MHz) of $[Sc(CH_2SiMe_3)_4][Li(thf)_4]$ (**6-Sc**) in $[D_8]$THF at 26 °C. The solvent residual signals are marked with asterisks.

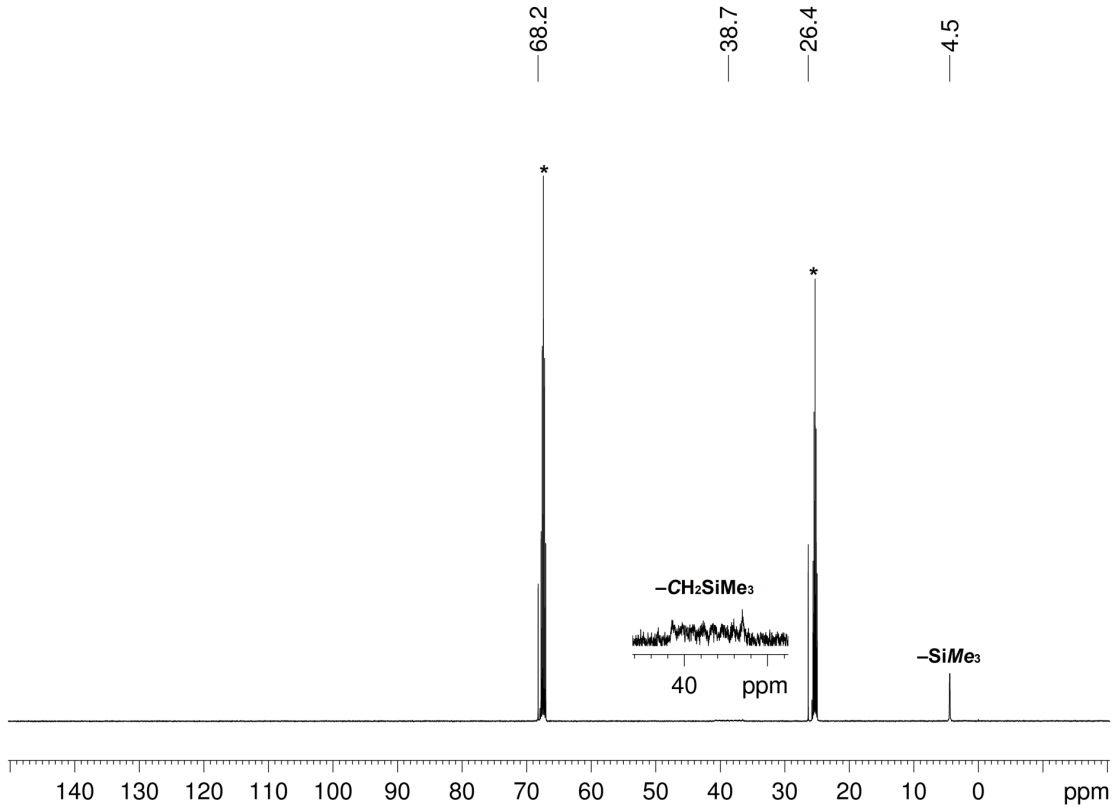

Figure S32. ^{13}C{^{1}H} NMR spectrum (126 MHz) of $[Sc(CH_2SiMe_3)_4][Li(thf)_4]$ (**6-Sc**) in $[D_8]$THF at 26 °C. The solvent residual signals are marked with asterisks.

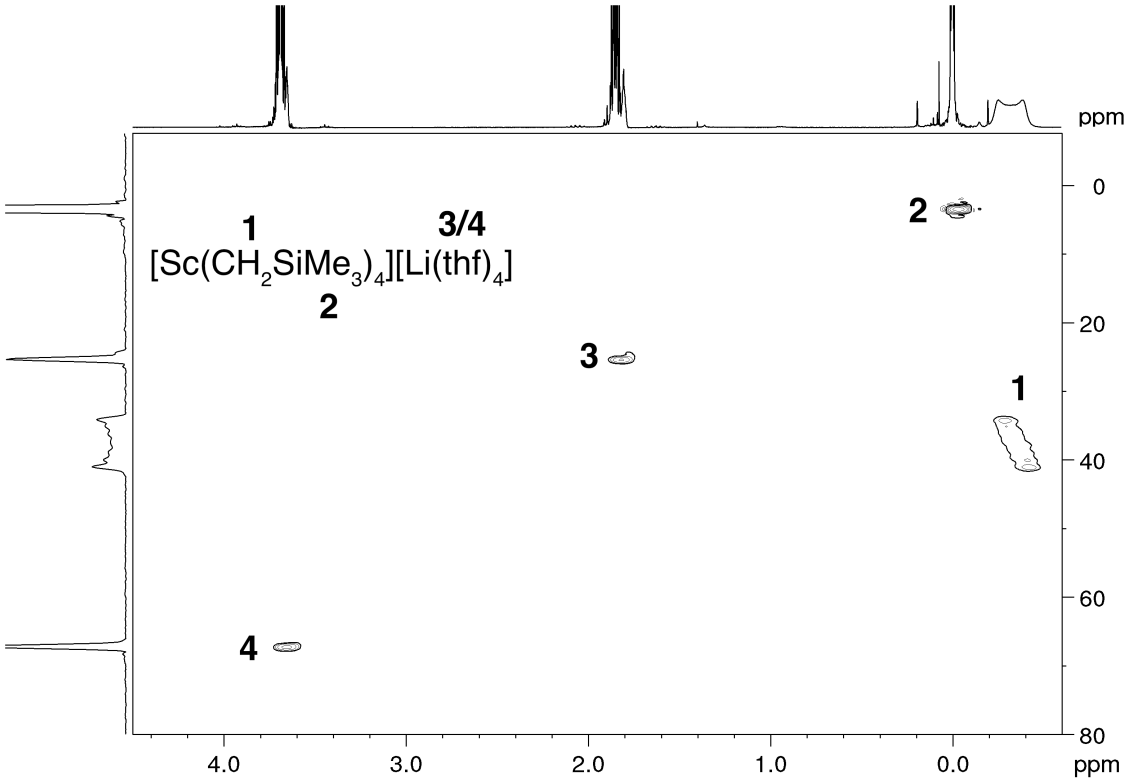

Figure S33. ^{1}H-^{13}C HSQC NMR spectrum of $[Sc(CH_2SiMe_3)_4][Li(thf)_4]$ (**6-Sc**) in $[D_8]THF$ at 26 °C.

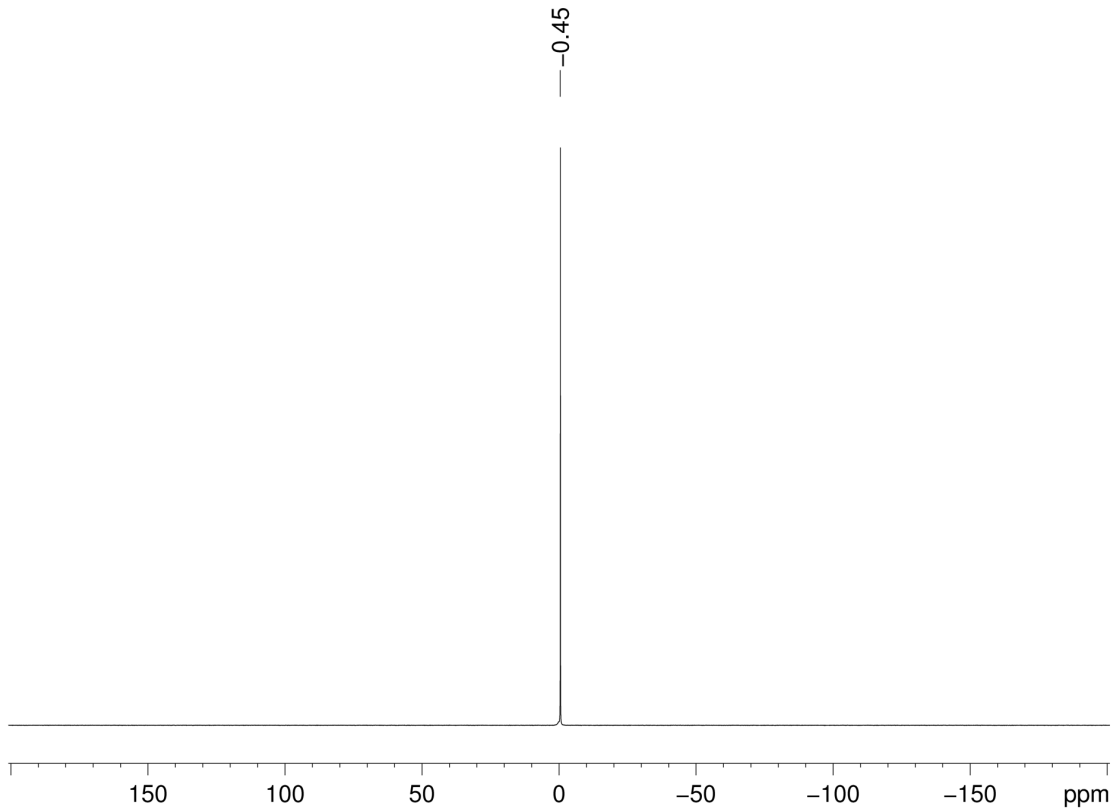

Figure S34. ^{7}Li NMR spectrum (194 MHz) of $[Sc(CH_2SiMe_3)_4][Li(thf)_4]$ (**6-Sc**) in $[D_8]THF$ at 26 °C.

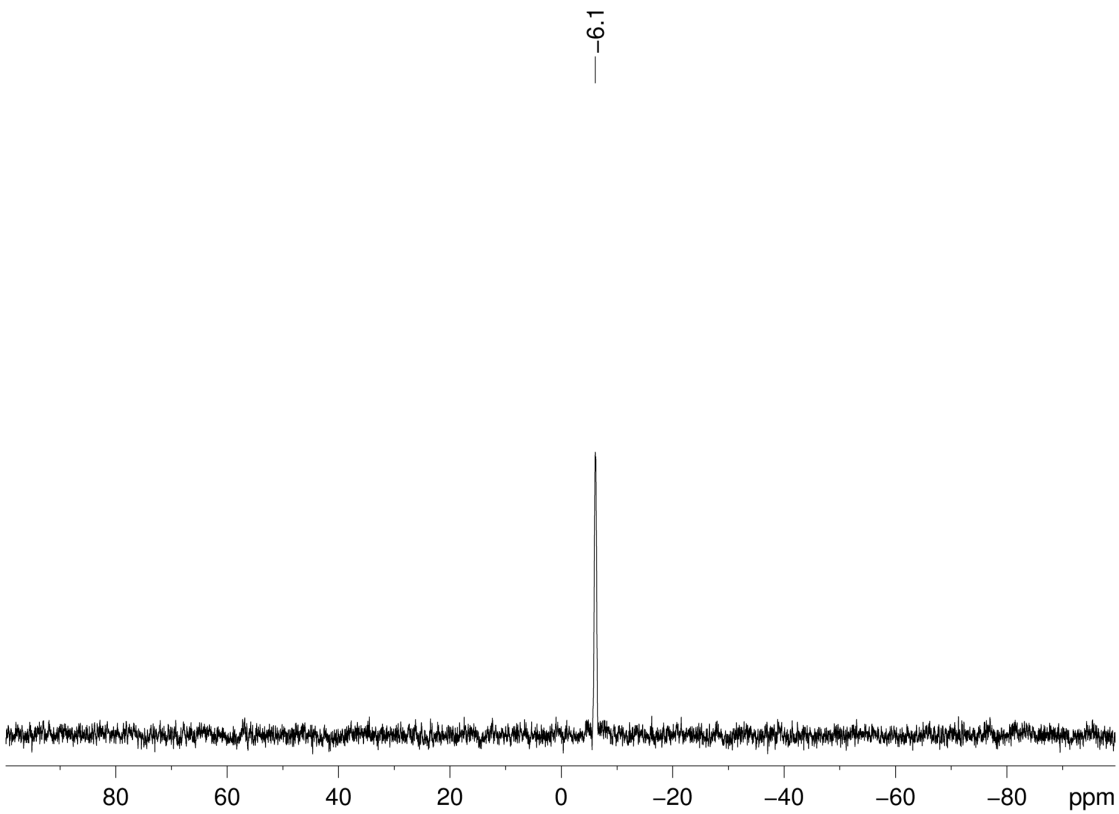

Figure S35. ^{29}Si NMR spectrum (60 MHz) of $[Sc(CH_2SiMe_3)_4][Li(thf)_4]$ (**6-Sc**) in $[D_8]$THF at 26 °C.

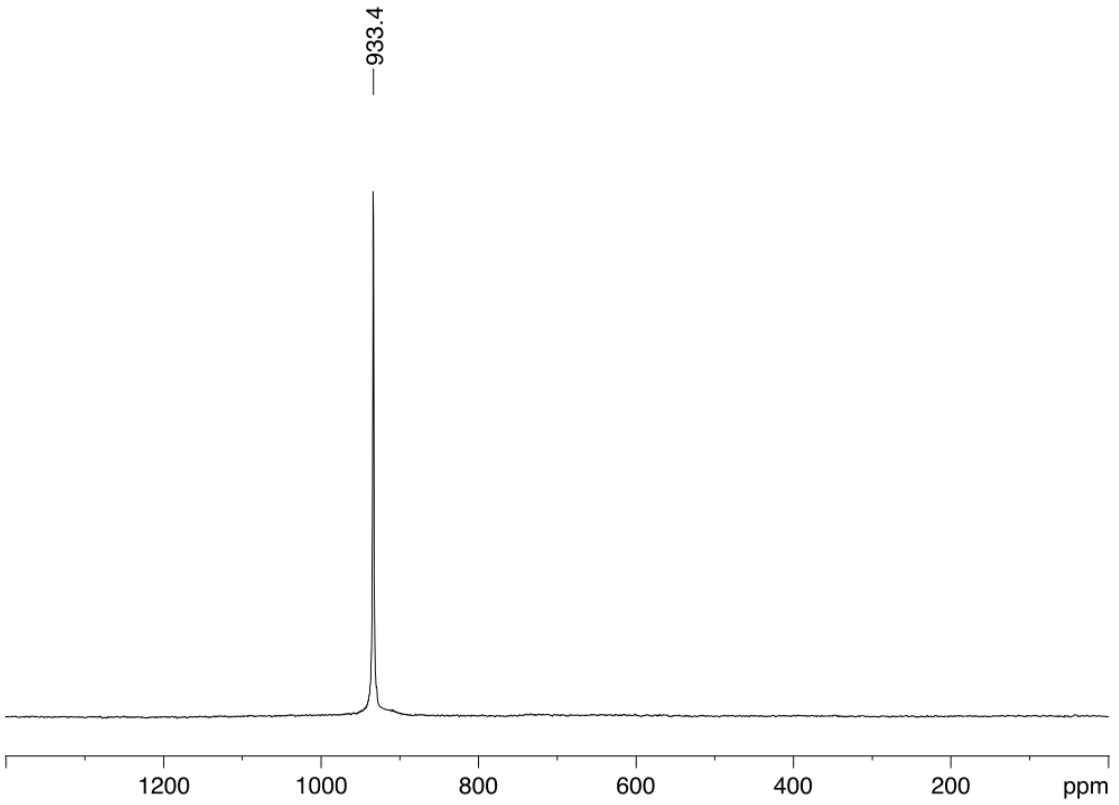

Figure S36. ^{45}Sc NMR spectrum (122 MHz) of $[Sc(CH_2SiMe_3)_4][Li(thf)_4]$ (**6-Sc**) in C_6D_6 at 26 °C.

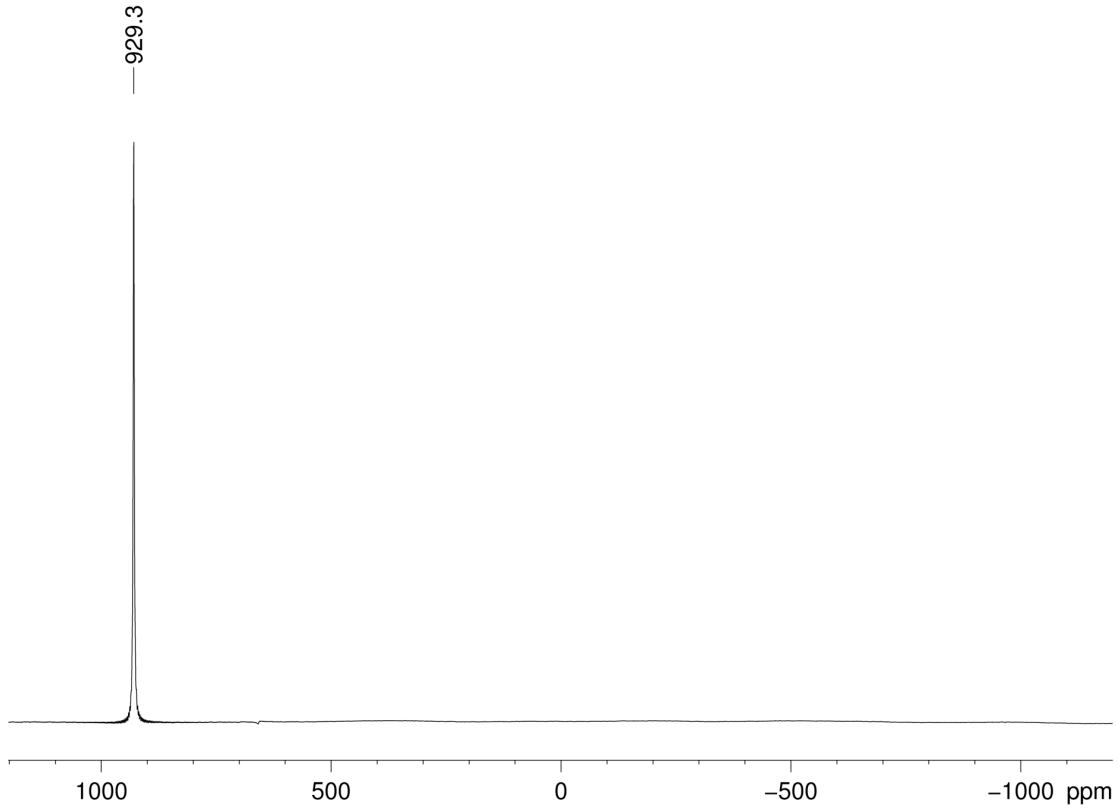

Figure S37. ^{45}Sc NMR spectrum (122 MHz) of $[Sc(CH_2SiMe_3)_4][Li(thf)_4]$ (**6-Sc**) in $[D_8]$THF at 26 °C.

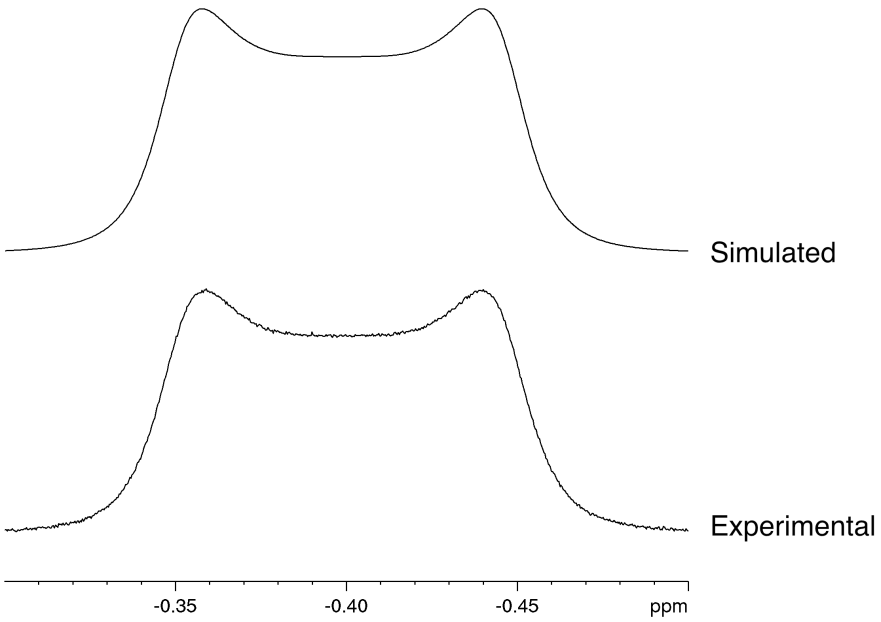

Figure S38. Comparison of simulated (top) and experimental (bottom) ^{1}H NMR spectrum (500 MHz) of $[Sc(CH_2SiMe_3)_4][Li(thf)_4]$ (**6-Sc**) in $[D_8]$THF at 26 °C (CH_2SiMe_3 peak range). The parameters of the simulated spectrum are: $\delta_{iso} = -0.399$ ppm, $J = 8.1$ Hz, coupled to: Sc-45, $T_1 = 0.036$ s.

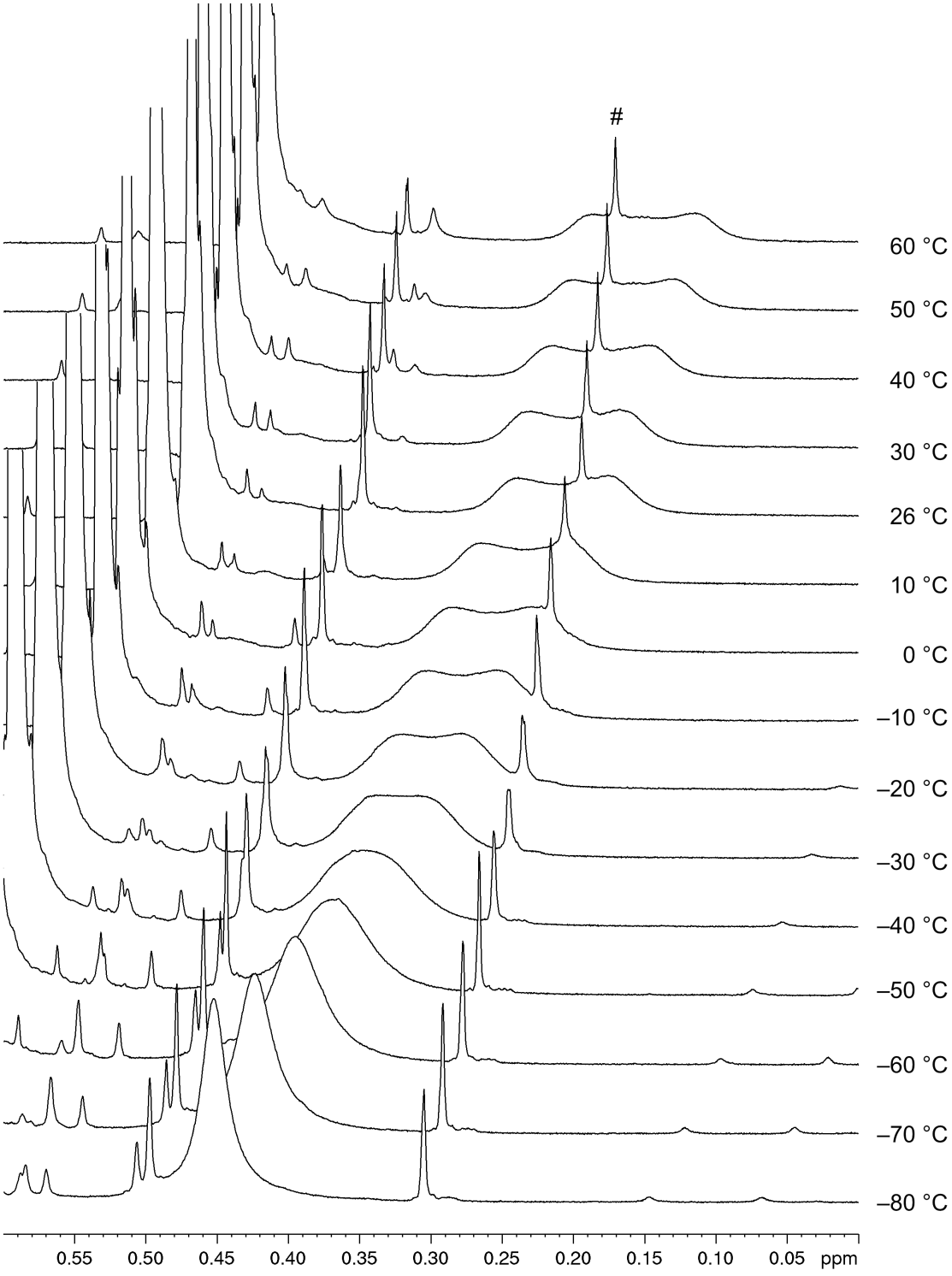

Figure S39. VT ^{1}H NMR spectrum (500 MHz) of $[Sc(CH_2SiMe_3)_4][Li(thf)_4]$ (**6-Sc**) in $[D_8]$THF. # is an unknown impurity.

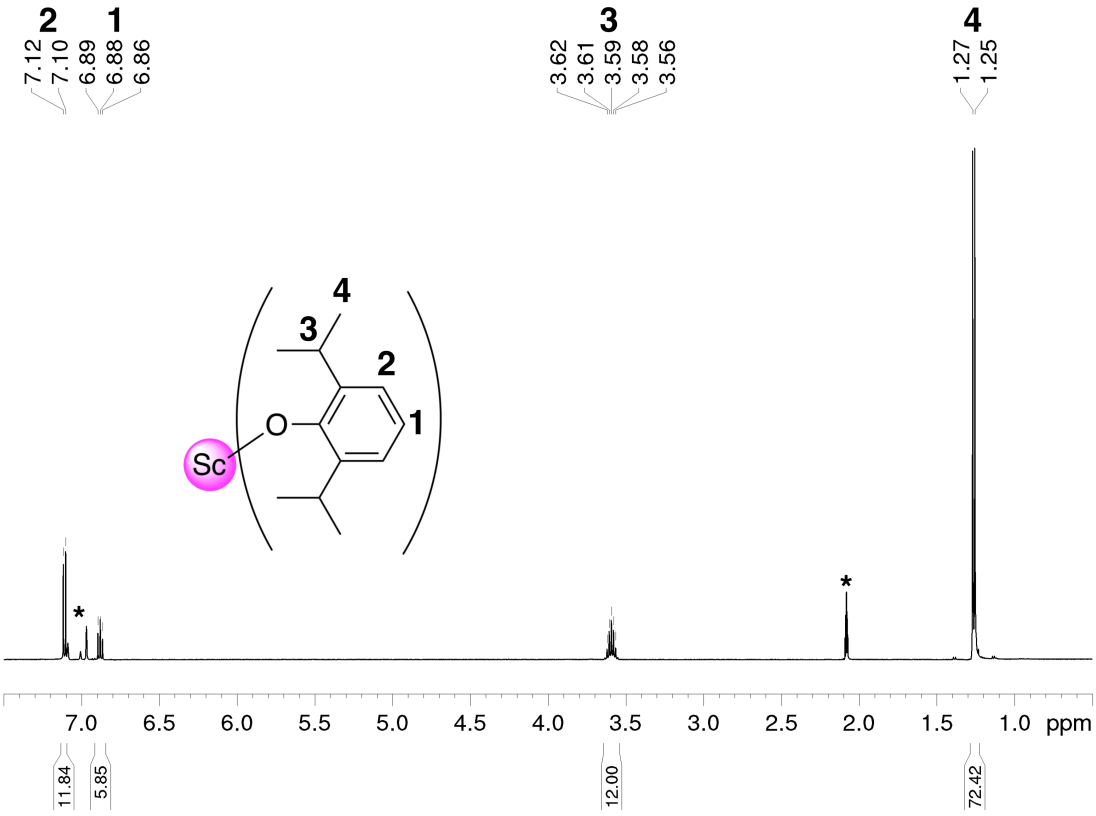

Figure S40. ^{1}H NMR spectrum (500 MHz) of [Sc(μ-OC$_6$H$_3$*i*Pr$_2$-2,6)(OC$_6$H$_3$*i*Pr$_2$-2,6)$_2$]$_2$ (**7**) in [D$_8$]toluene at 26 °C. The solvent residual signals are marked with an asterisk.

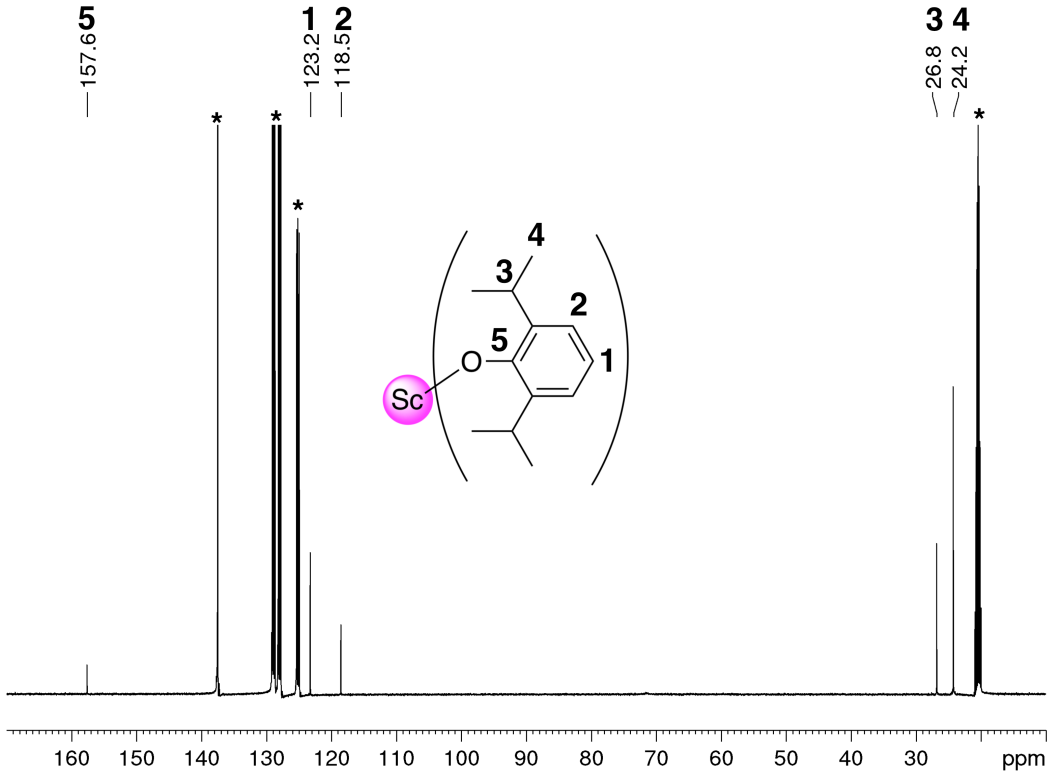

Figure S41. ^{13}C{^{1}H} NMR spectrum (126 MHz) of Sc(μ-OC$_6$H$_3$*i*Pr$_2$-2,6)(OC$_6$H$_3$*i*Pr$_2$-2,6)$_2$]$_2$ (**7**) in [D$_8$]toluene at 26 °C. The solvent residual signals are marked with an asterisk.

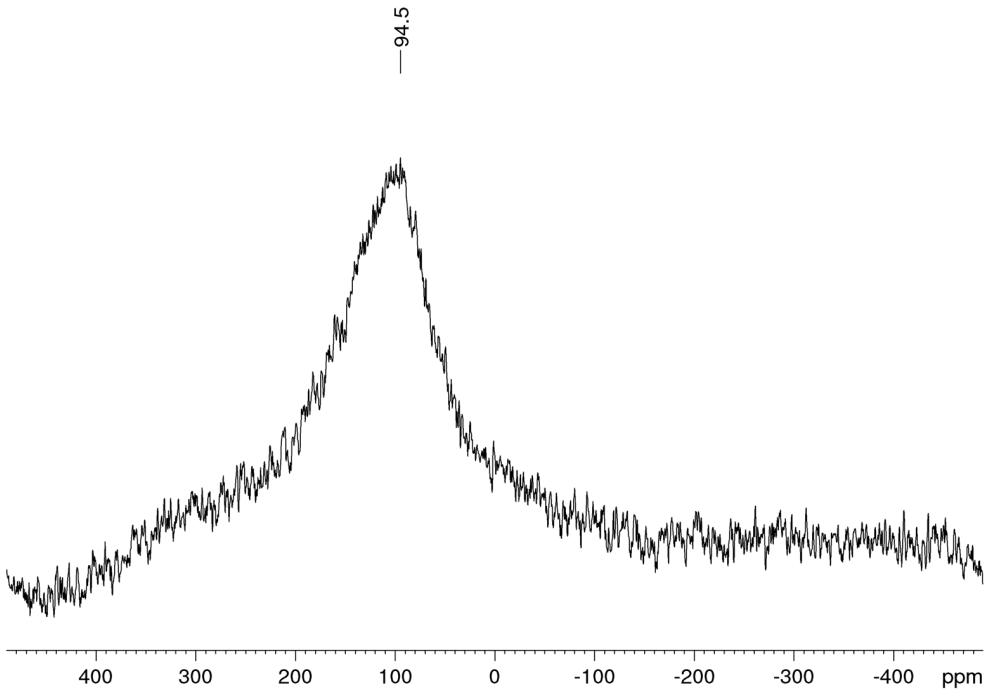

Figure S42. ^{45}Sc NMR spectrum (122 MHz) of [Sc(μ-OC$_6$H$_3$*i*Pr$_2$-2,6)(OC$_6$H$_3$*i*Pr$_2$-2,6)$_2$]$_2$ (**7**) in [D$_8$]toluene at 26 °C.

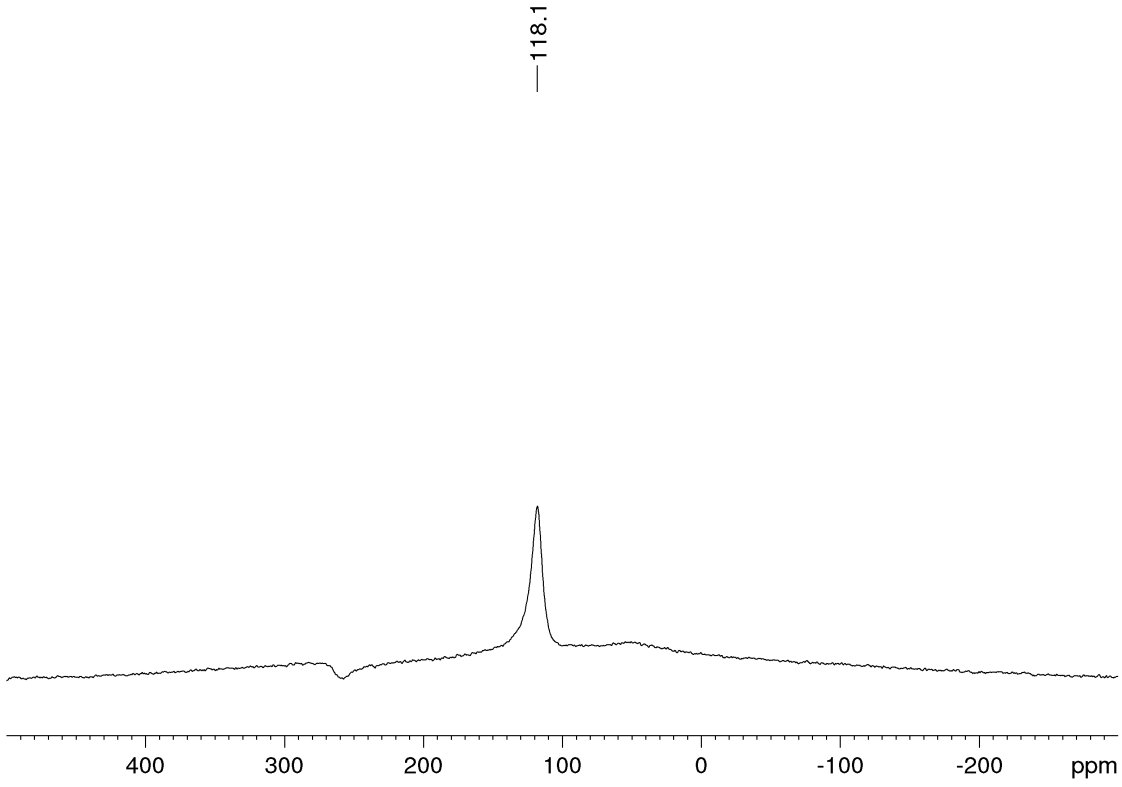

Figure S43. ^{45}Sc NMR spectrum (122 MHz) of Sc(μ-OC$_6$H$_3$*i*Pr$_2$-2,6)(OC$_6$H$_3$*i*Pr$_2$-2,6)$_2$]$_2$ (**7**) in [D$_8$]THF at 26 °C.

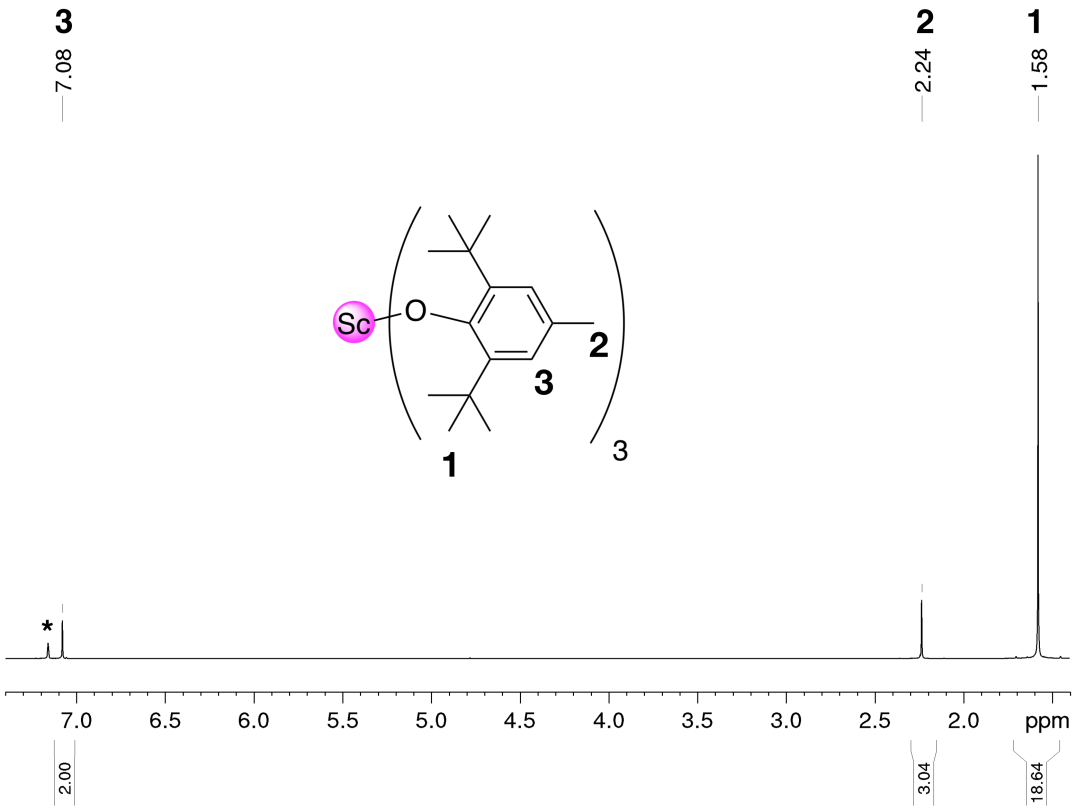

Figure S44. ^{1}H NMR spectrum (500 MHz) of Sc(OC$_6$H$_2$-*t*Bu$_2$-2,6-Me-4)$_3$ in C$_6$D$_6$ at 26 °C. The solvent residual signal is marked with an asterisk.

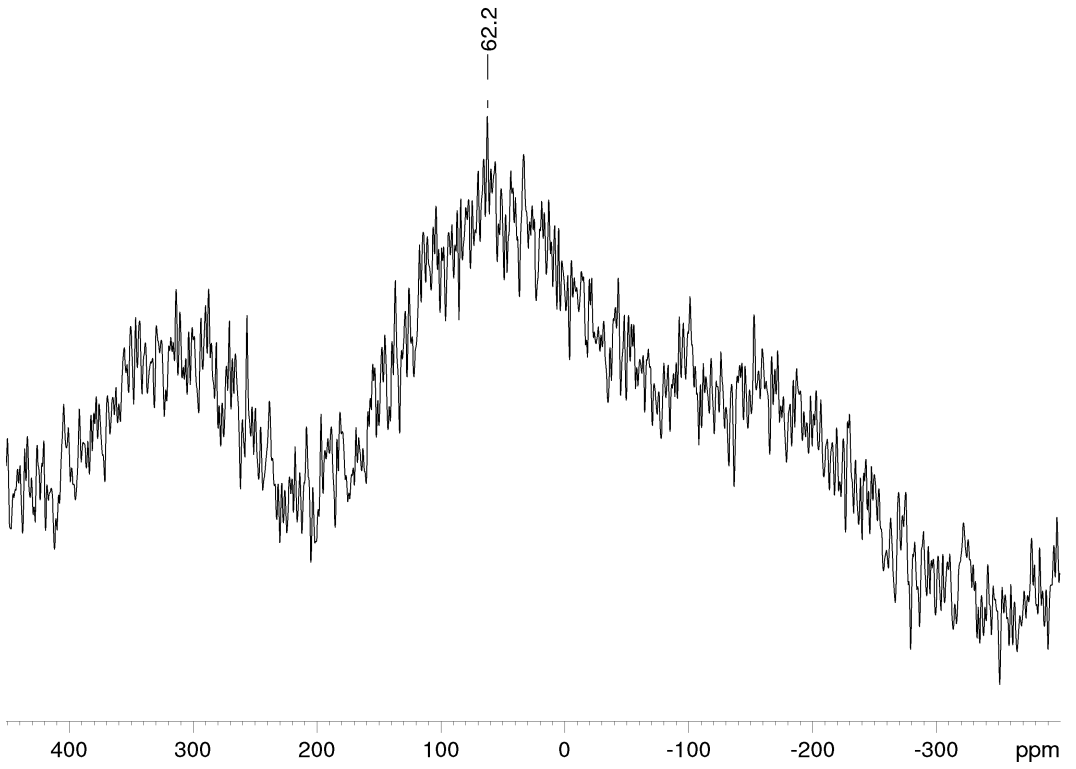

Figure S45. ^{45}Sc NMR spectrum (122 MHz) of Sc(OC$_6$H$_2$-*t*Bu$_2$-2,6-Me-4)$_3$ in C$_6$D$_6$ at 26 °C.

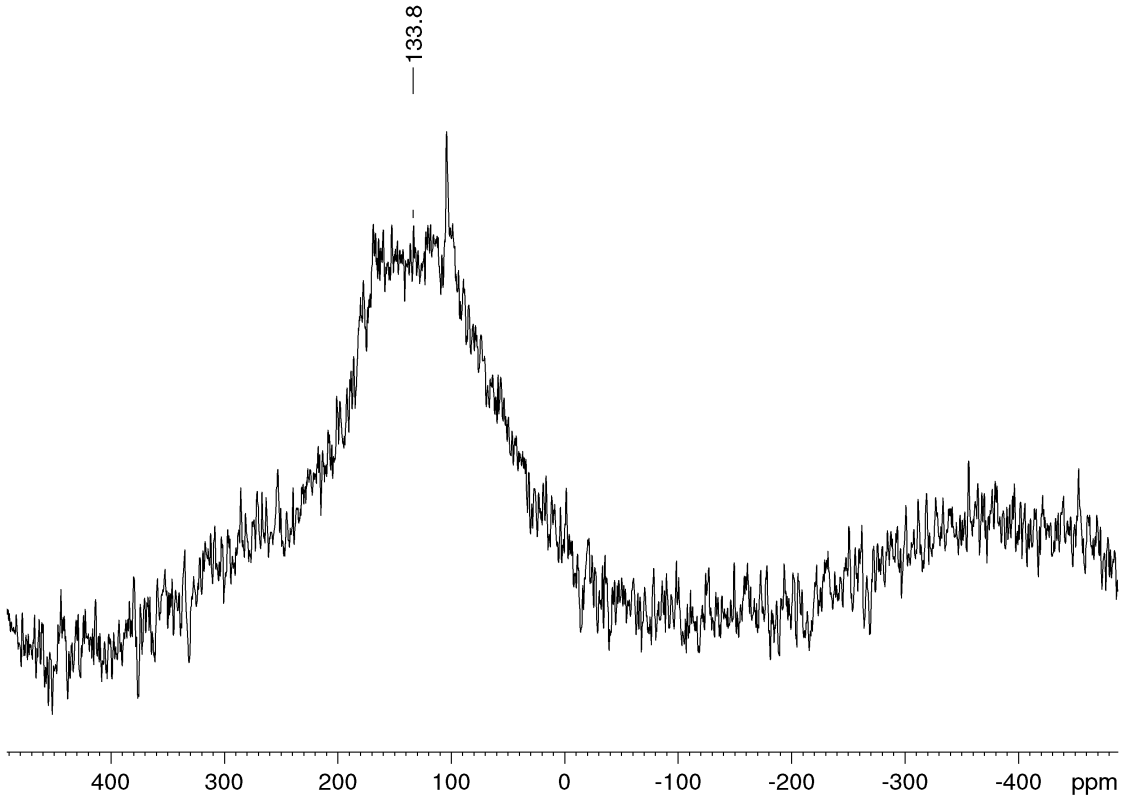

Figure S46. ^{45}Sc NMR spectrum (122 MHz) of Sc(OC$_6$H$_2$-*t*Bu$_2$-2,6-Me-4)$_3$ in [D$_8$]THF at 26 °C.

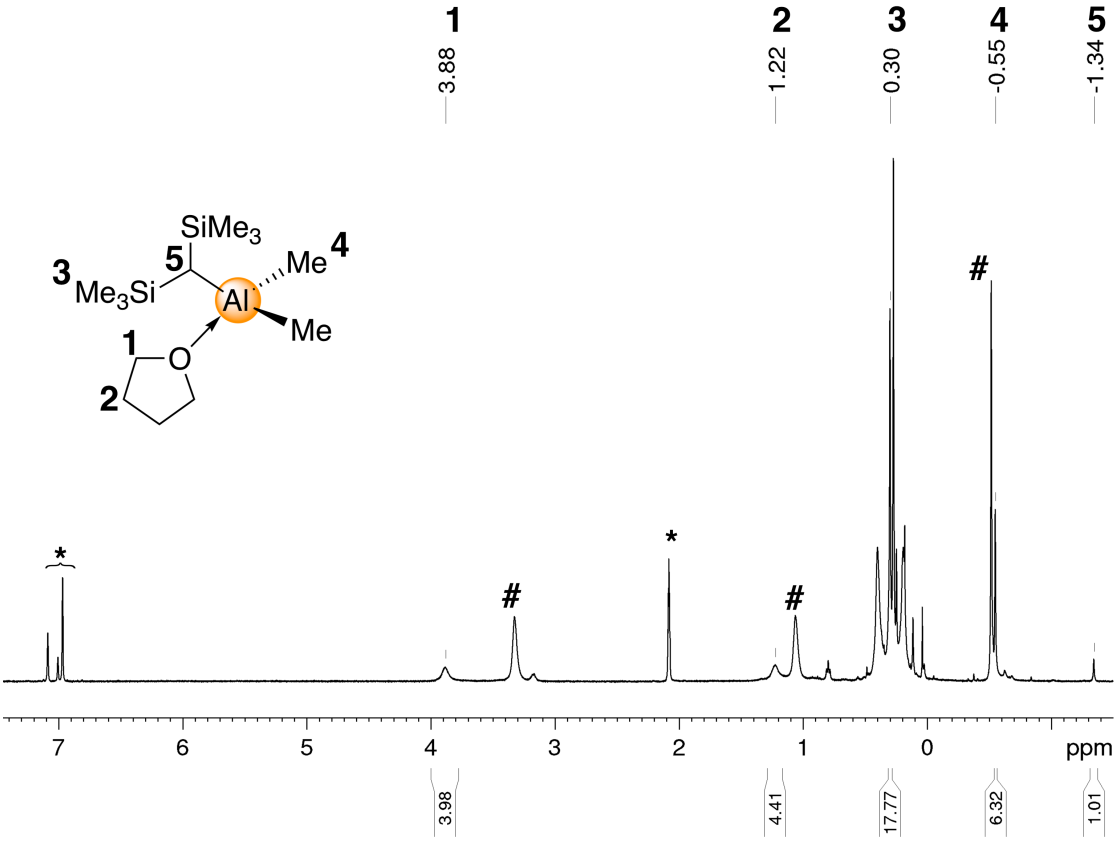

Figure S47. ^{1}H NMR spectrum (500 MHz) of the reaction of complex **4** with 4 equiv. AlMe$_3$ in [D$_8$]toluene at 26 °C. Signals of *in situ* formed complex **5** labelled with numbers. Presumed signals of AlMe$_3$·thf marked with #, the solvent residual signal is marked with an asterisk.

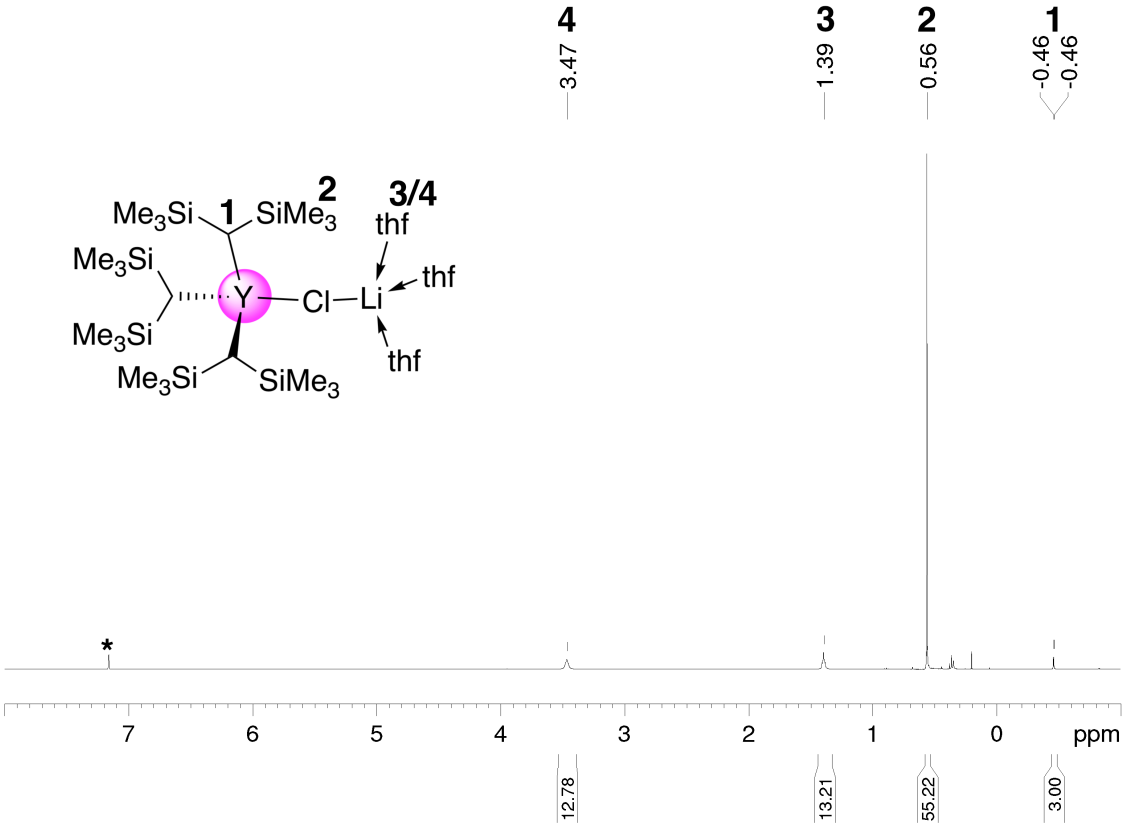

Figure S48. ^{1}H NMR spectrum (500 MHz) of Y[CH(SiMe$_3$)$_2$]$_3$(μ-Cl)Li(thf)$_3$ (**2-Y**) in C_6D_6 at 26 °C. The solvent residual signal is marked with an asterisk.

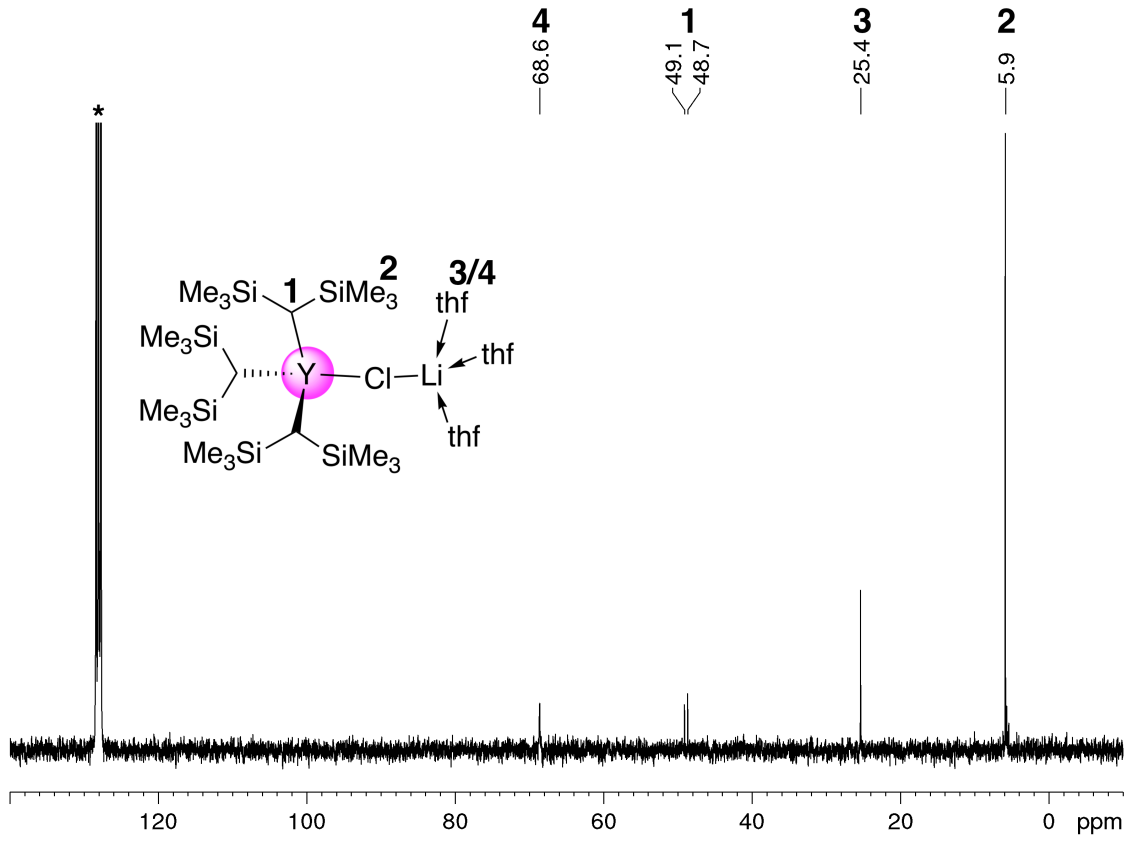

Figure S49. ^{13}C{^{1}H} NMR spectrum (126 MHz) of Y[CH(SiMe$_3$)$_2$]$_3$(μ-Cl)Li(thf)$_3$ (**2-Y**) in C_6D_6 at 26 °C. The solvent residual signal is marked with an asterisk.

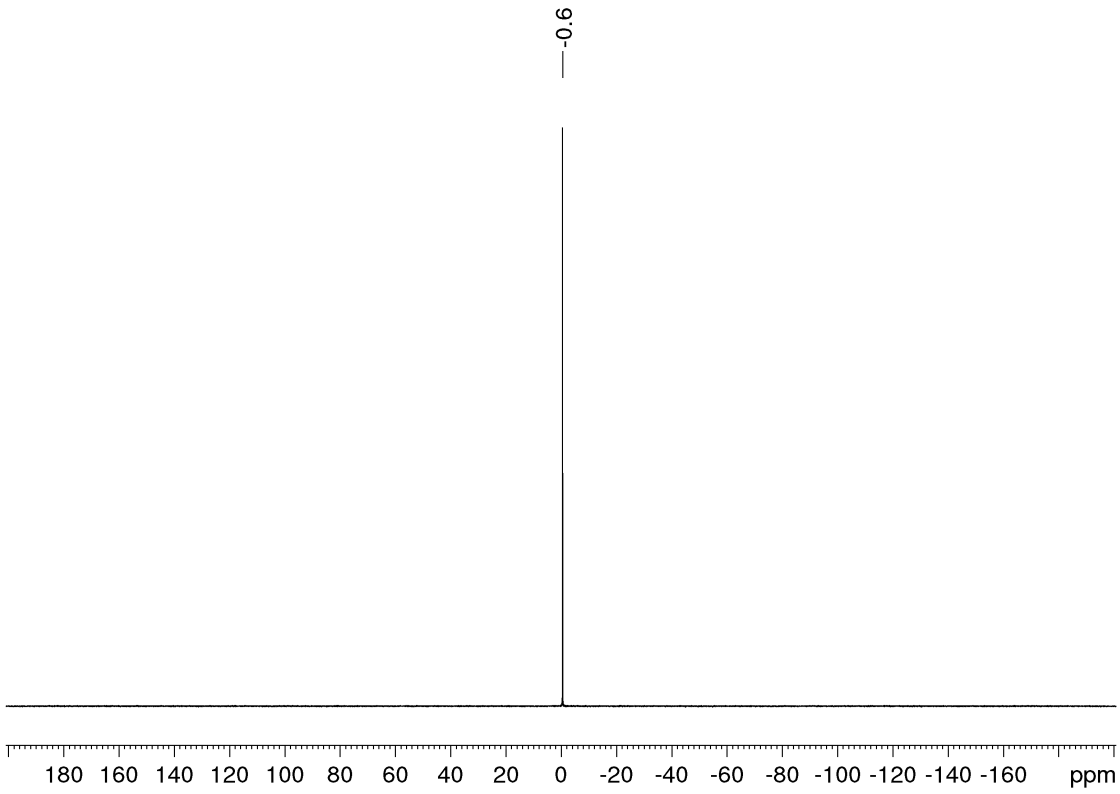

Figure S50. $^{7}Li\{^{1}H\}$ NMR spectrum (194 MHz) of $Y[CH(SiMe_3)_2]_3(\mu\text{-}Cl)Li(thf)_3$ (**2-Y**) in C_6D_6 at 26 °C.

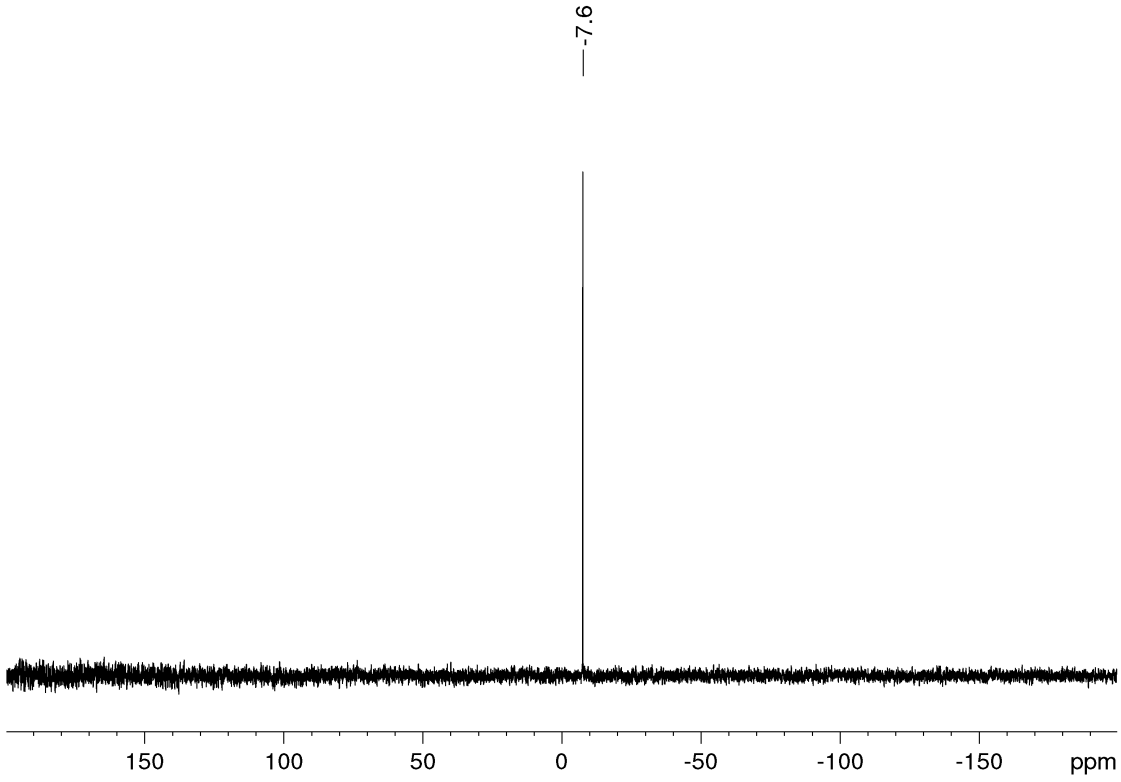

Figure S51. ^{29}Si INEPT NMR spectrum (60 MHz) of $Y[CH(SiMe_3)_2]_3(\mu\text{-}Cl)Li(thf)_3$ (**2-Y**) in C_6D_6 at 26 °C.

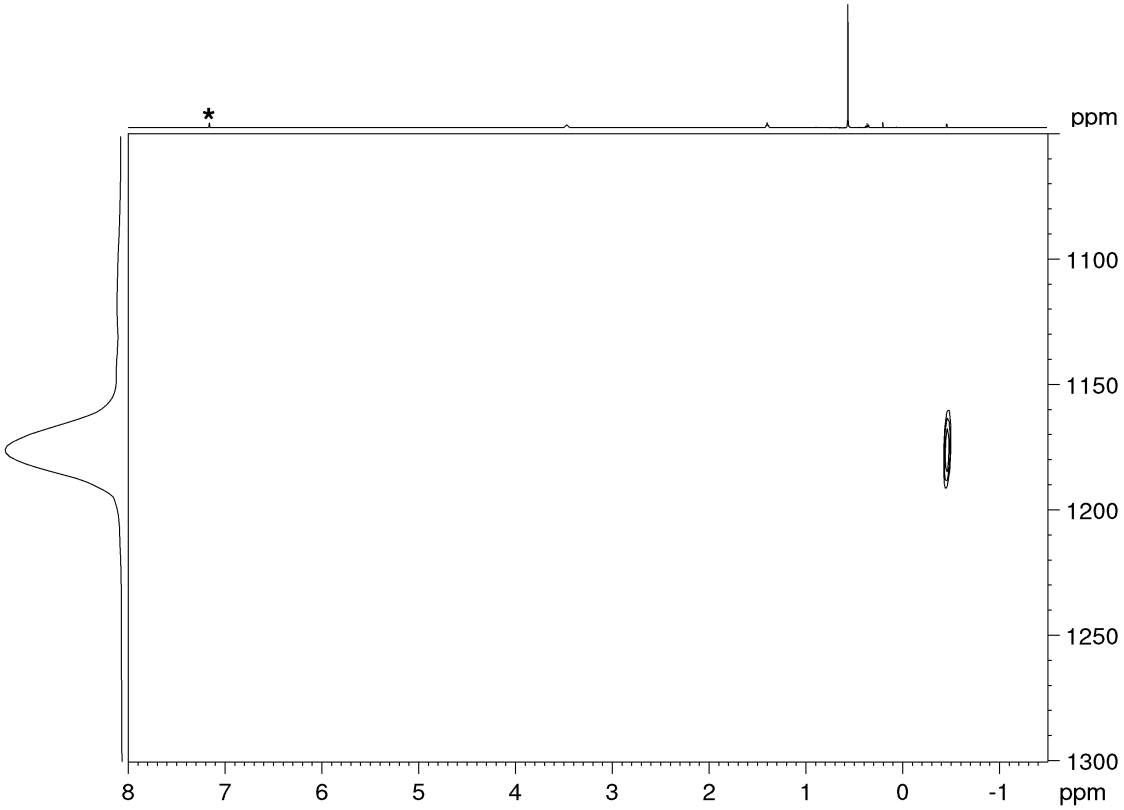

Figure S52. $^{1}H–^{89}Y$ HSQC NMR spectrum (25 MHz) of $Y[CH(SiMe_3)_2]_3(\mu\text{-}Cl)Li(thf)_3$ (**2-Y**) in C_6D_6 at 26 °C. The solvent residual signal is marked with an asterisk.

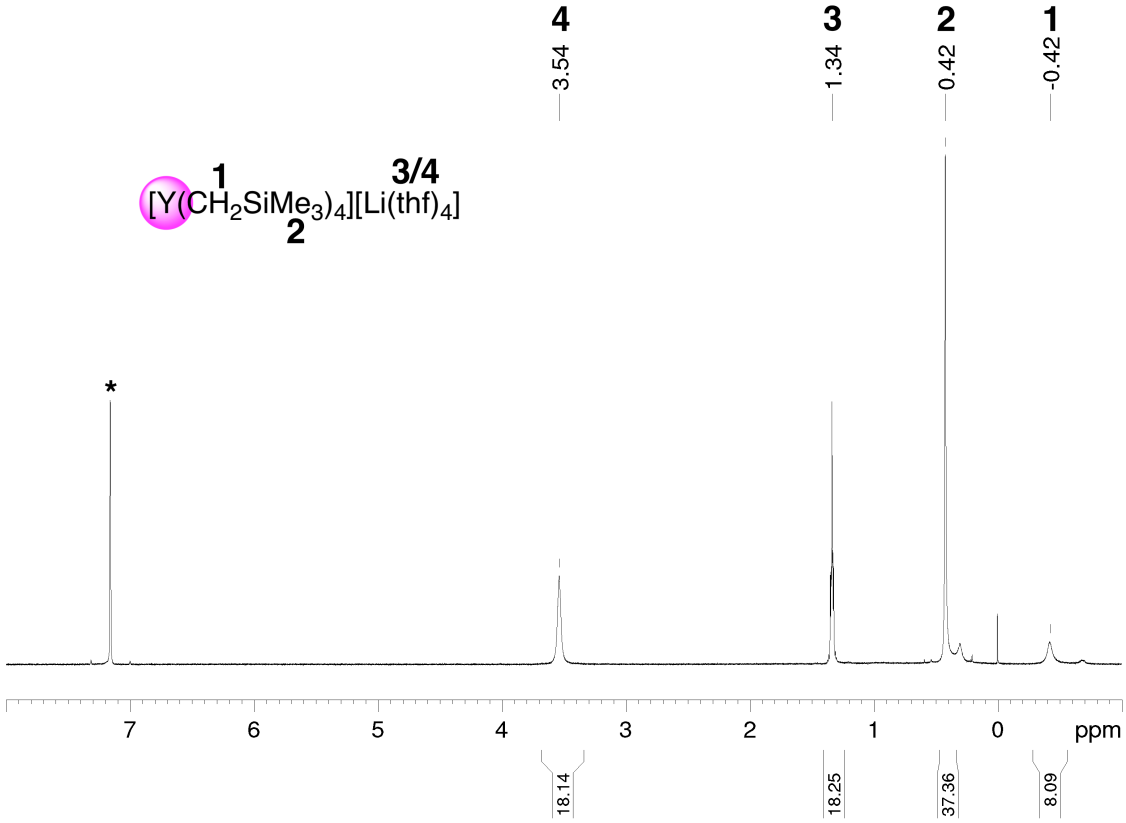

Figure S53. ^{1}H NMR spectrum (500 MHz) of $[Y(CH_2SiMe_3)_4][Li(thf)_4]$ (**6-Y**) in C_6D_6 at 26 °C. The solvent residual signal is marked with an asterisk.

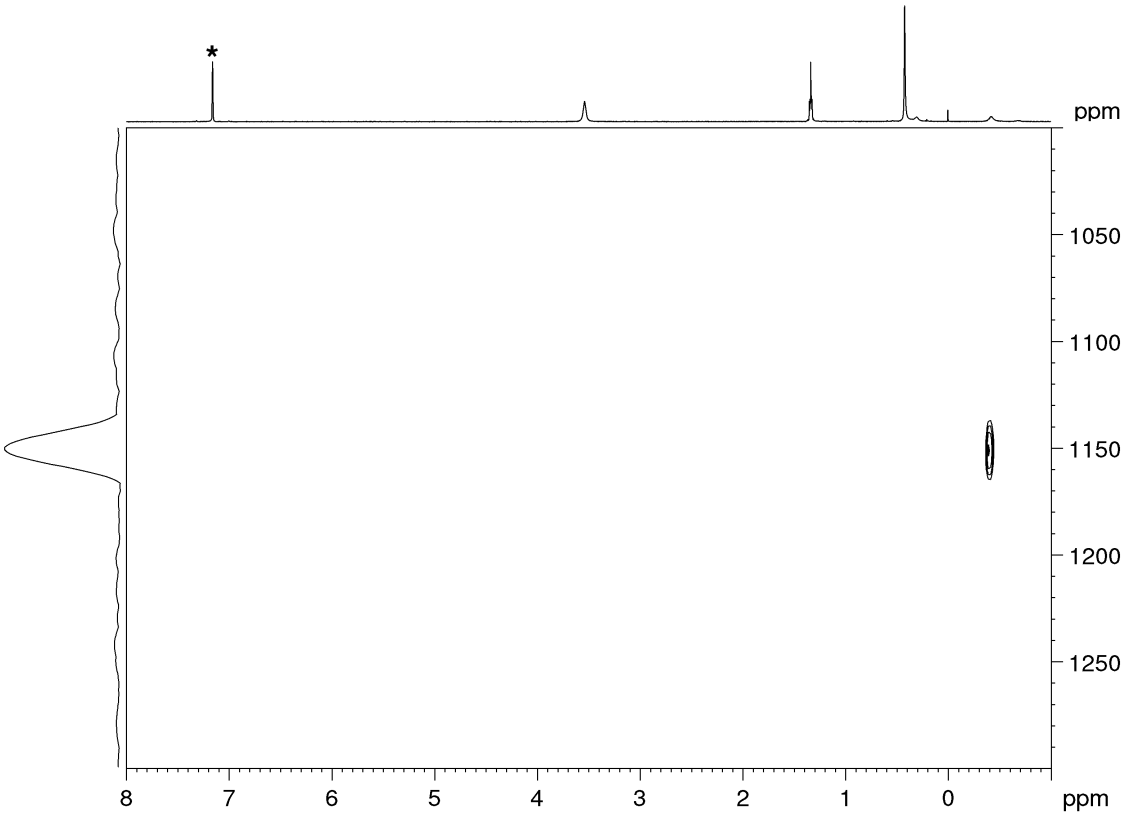

Figure S54. ^{1}H–^{89}Y HSQC NMR spectrum (25 MHz) of $[Y(CH_2SiMe_3)_4][Li(thf)_4]$ (**6-Y**) in C_6D_6 at 26 °C. The solvent residual signal is marked with an asterisk.

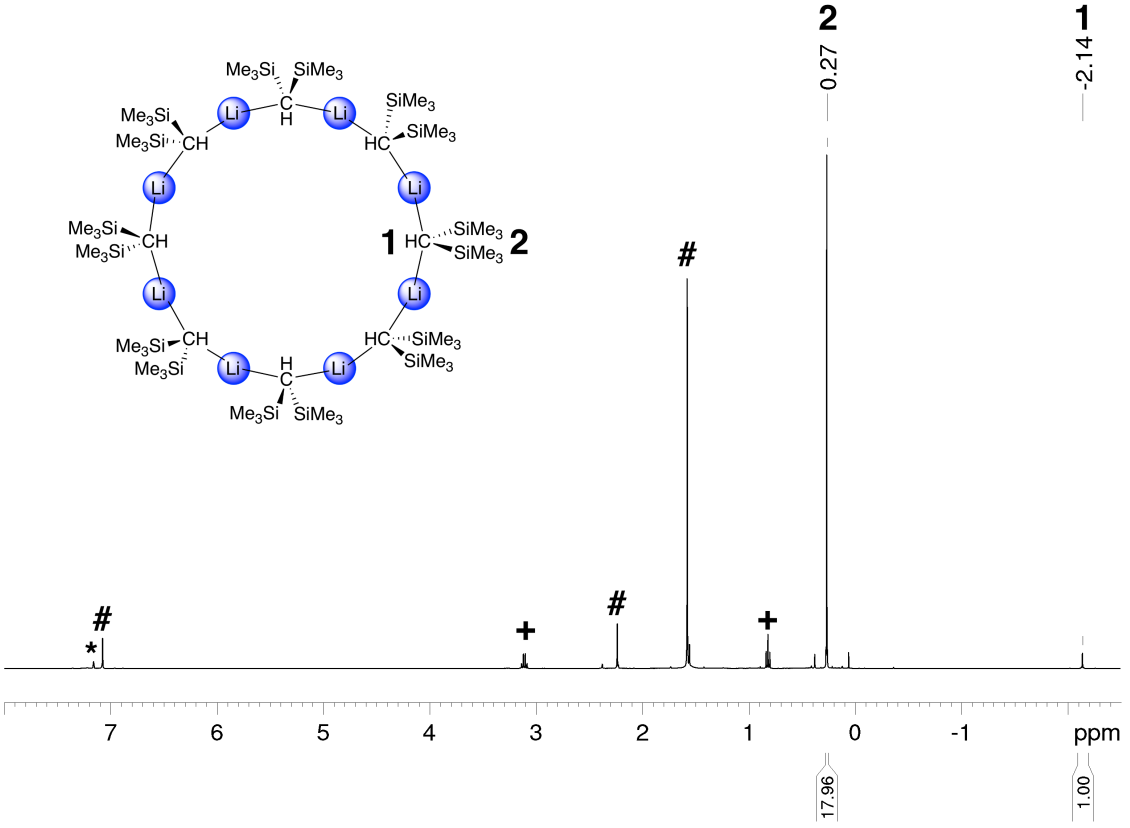

Figure S55. ^{1}H NMR spectrum (400 MHz) of $[Li\{CH(SiMe_3)_2\}]_8$ in C_6D_6 at 26 °C. Residual diethyl ether is marked with a +, unreacted $Sc(OC_6H_2$-*t*Bu_2-2,6-Me-4$)_3$ is marked with a #. The solvent residual signal is marked with an asterisk.

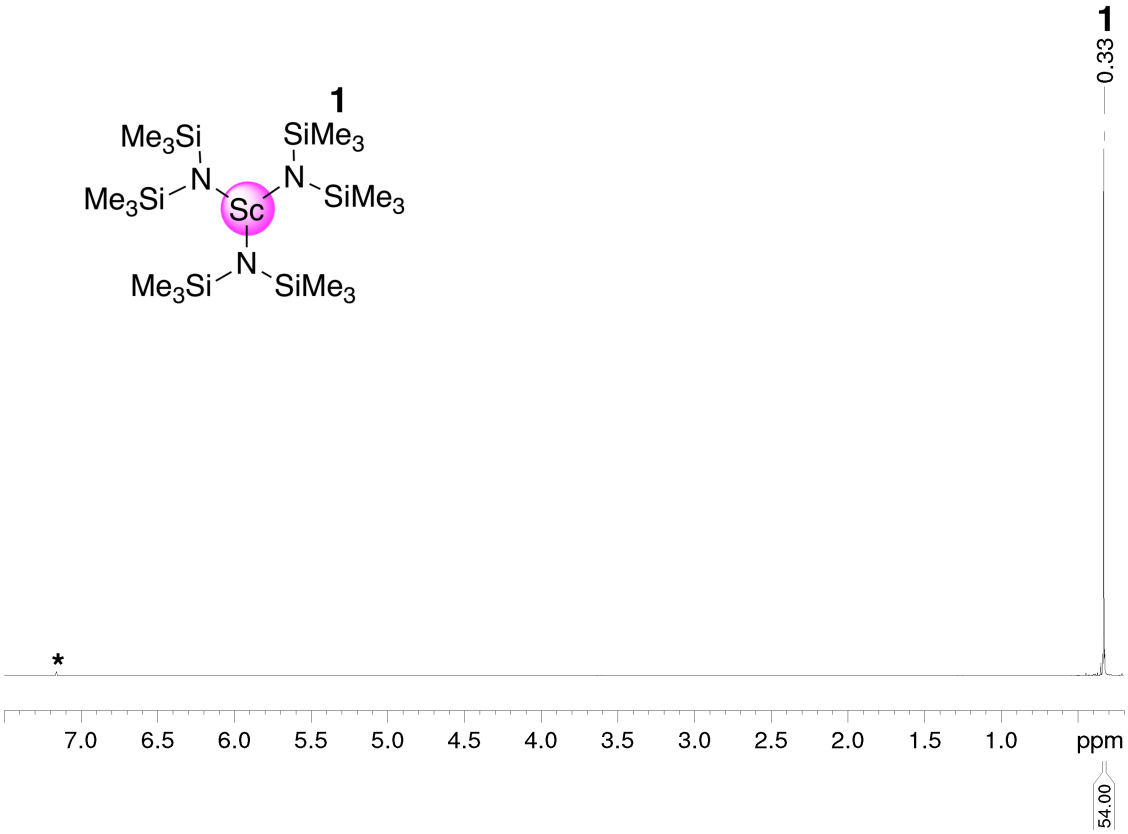

Figure S56. ^{1}H NMR spectrum (500 MHz) of $Sc[N(SiMe_3)_2]_3$ in C_6D_6 at 26 °C. The solvent residual signal is marked with an asterisk.

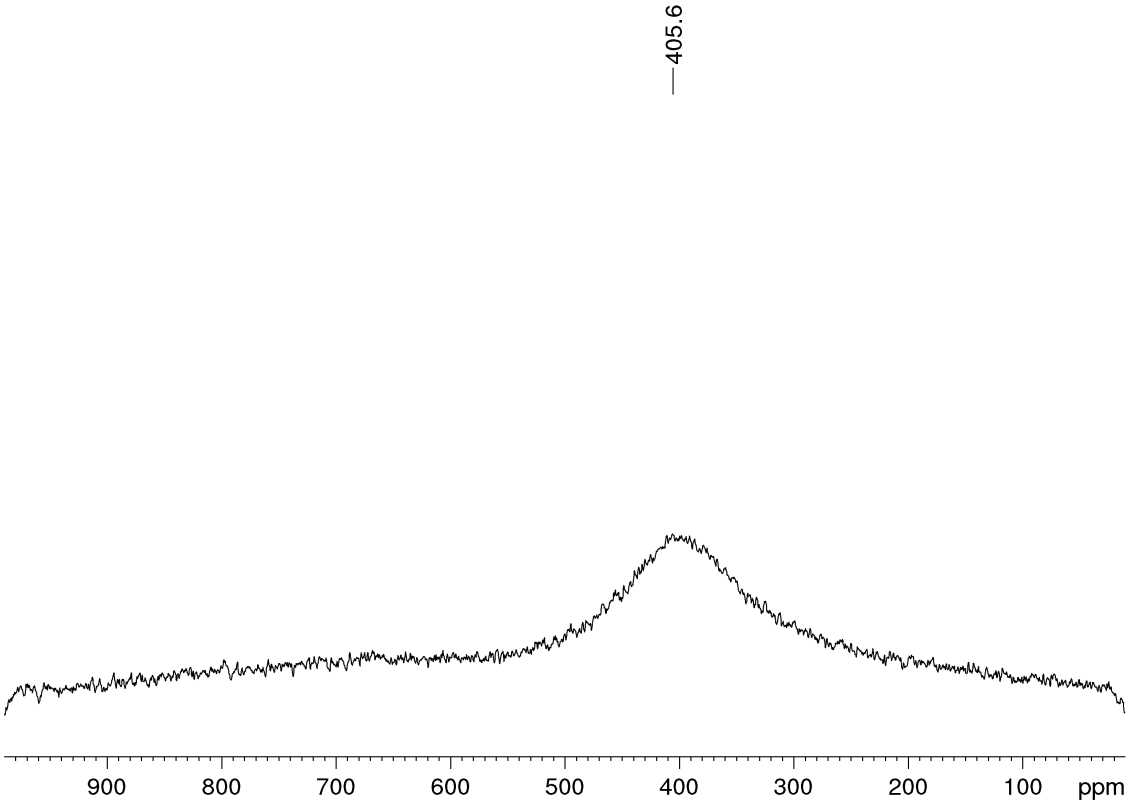

Figure S57. ^{45}Sc NMR spectrum (122 MHz) of $Sc[N(SiMe_3)_2]_3$ in C_6D_6 at 26 °C.

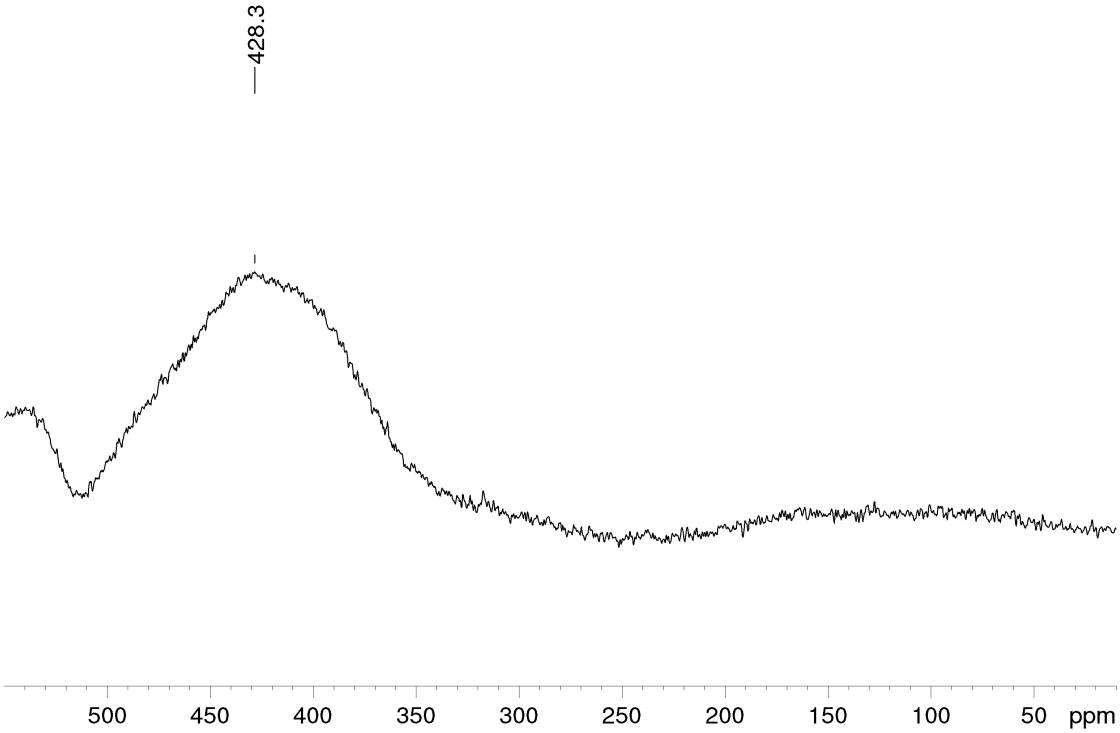

Figure S58. ^{45}Sc NMR spectrum (122 MHz) of $Sc[N(SiMe_3)_2]_3$ in $[D_8]THF$ at 26 °C.

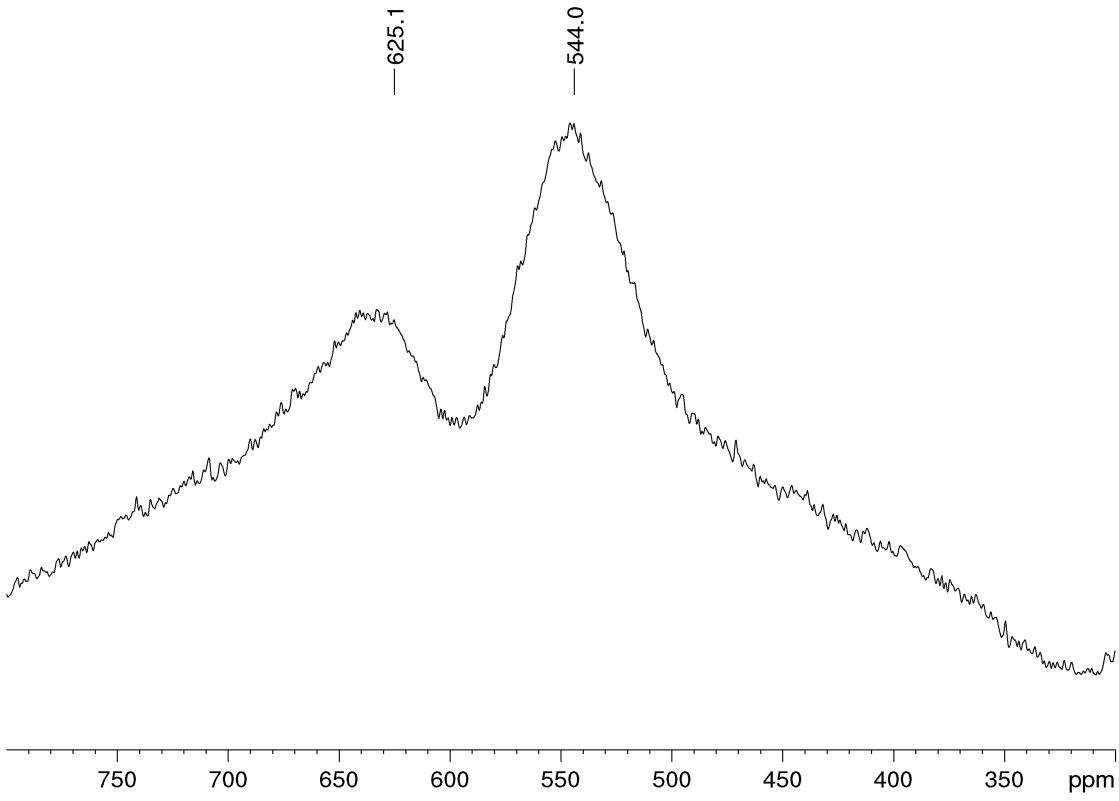

Figure S59. ^{45}Sc NMR spectrum (122 MHz) of the reaction of $[Sc(\mu\text{-}OC_6H_3iPr_2\text{-}2,6)(OC_6H_3iPr_2\text{-}2,6)_2]_2$ (**7**) with 3 equivalents of $Li[CH(SiMe_3)_2]$ in C_6D_6 at 26 °C.

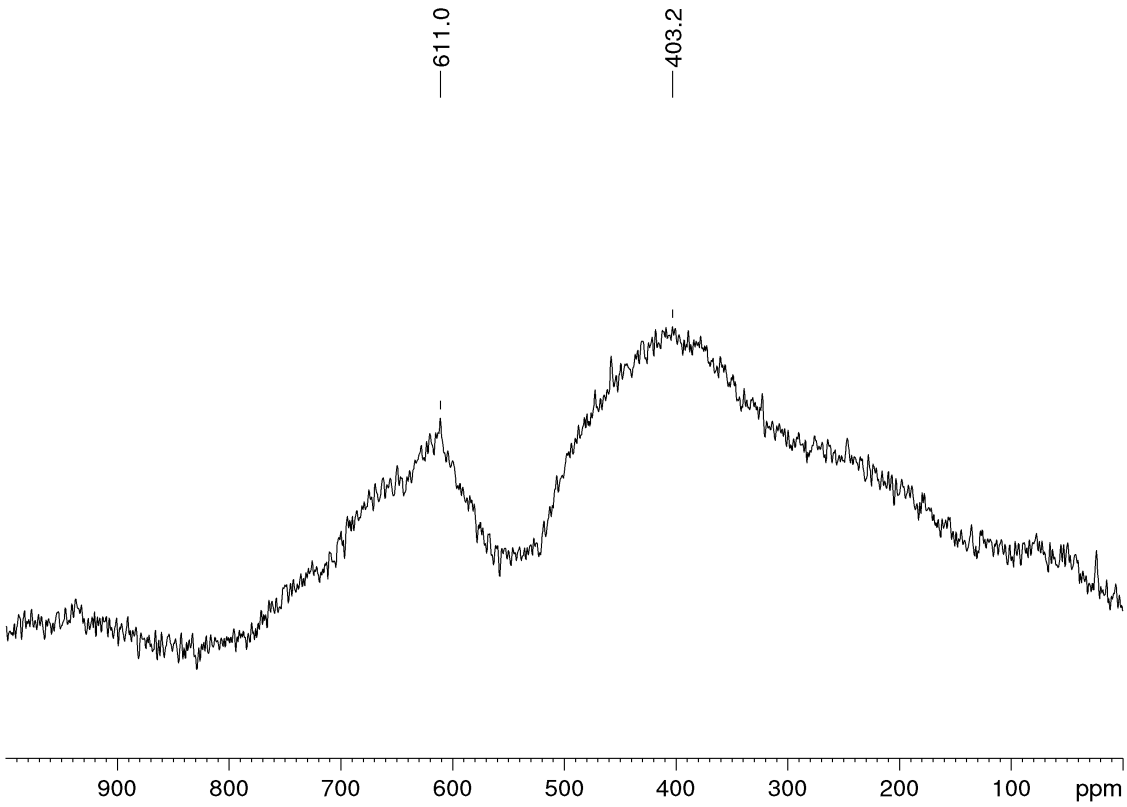

Figure S60. ^{45}Sc NMR spectrum (122 MHz) of the reaction of $Sc(OC_6H_2$-*t*Bu_2-2,6-Me-4$)_3$ with 3 equivalents of $Li[CH(SiMe_3)_2]$ after heating for 18 h to 40 °C in C_6D_6 at 26 °C.

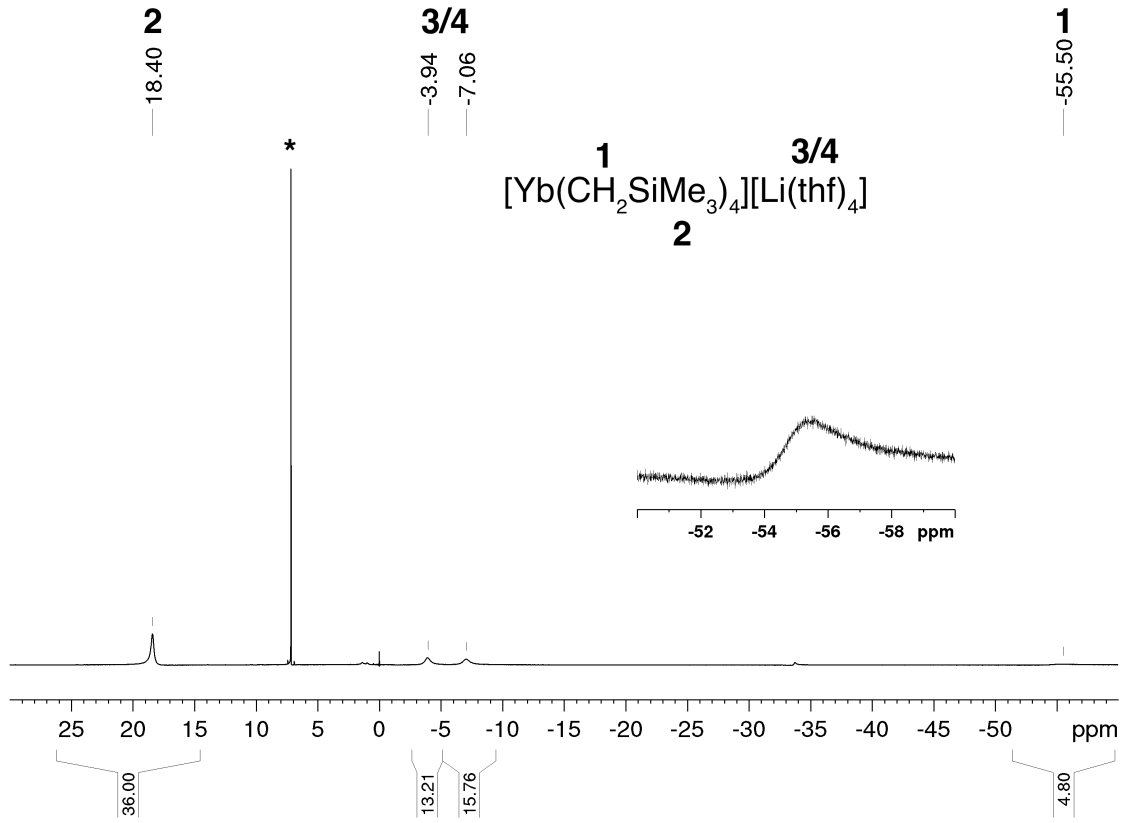

Figure S61. ^{1}H NMR spectrum (400 MHz) of $[Yb(CH_2SiMe_3)_4][Li(thf)_4]$ (**6-Yb**) in C_6D_6 at 26 °C. Solvent residual peak is marked with an asterisk.

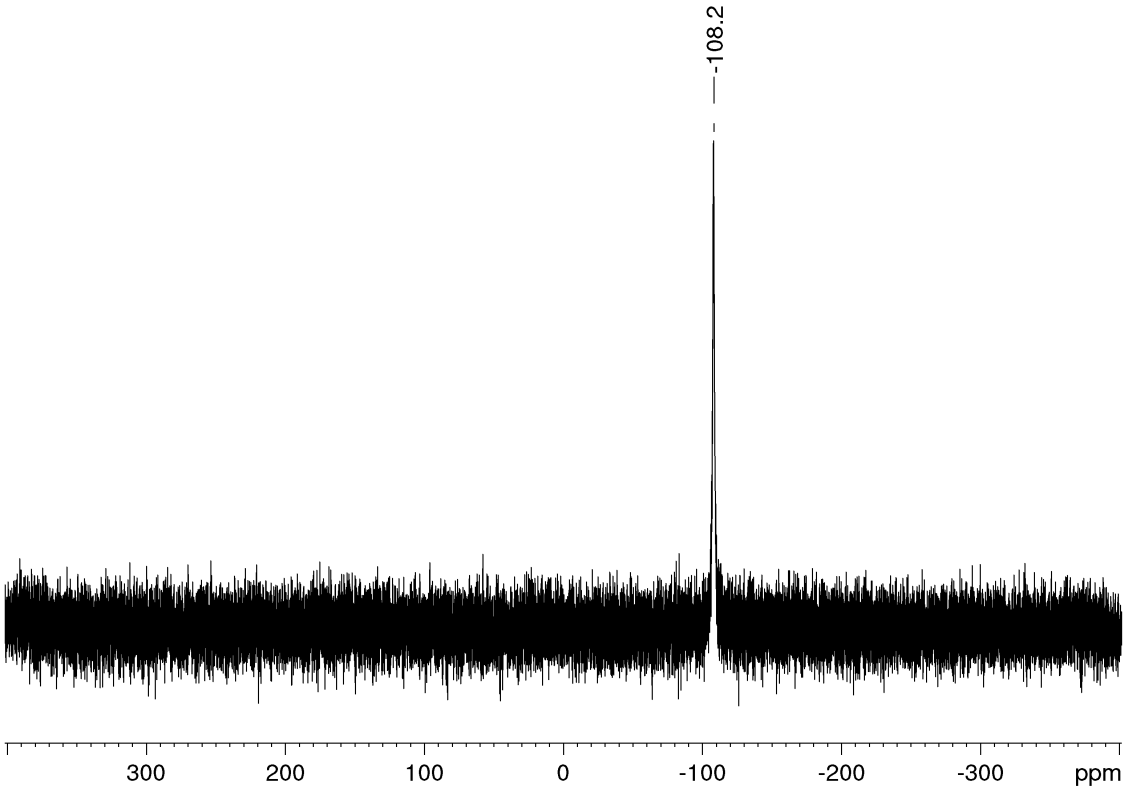

Figure S62. ^{7}Li NMR spectrum (117 MHz) of $[Yb(CH_2SiMe_3)_4][Li(thf)_4]$ (**6-Yb**) in C_6D_6 at 26 °C. Solvent residual peak is marked with an asterisk.

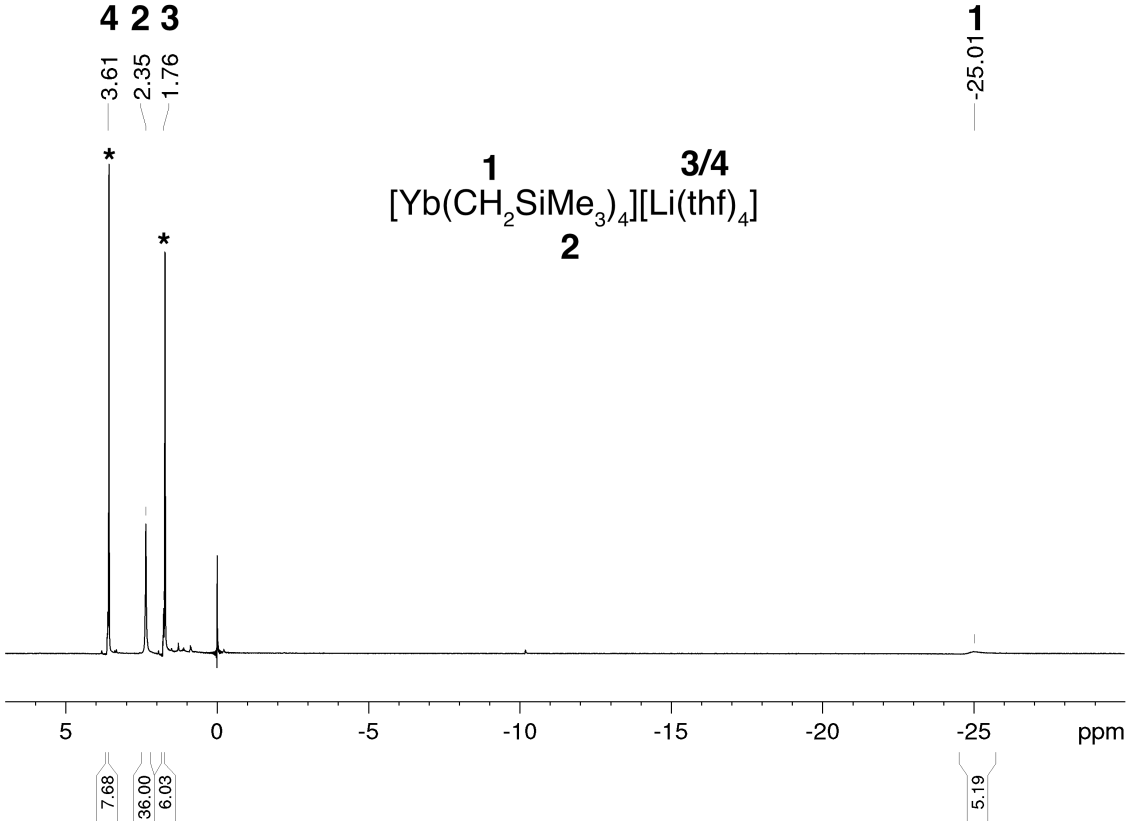

Figure S63. ^{1}H NMR spectrum (400 MHz) of $[Yb(CH_2SiMe_3)_4][Li(thf)_4]$ (**6-Yb**) in $[D_8]$THF at 26 °C. Solvent residual peaks are marked with asterisks.

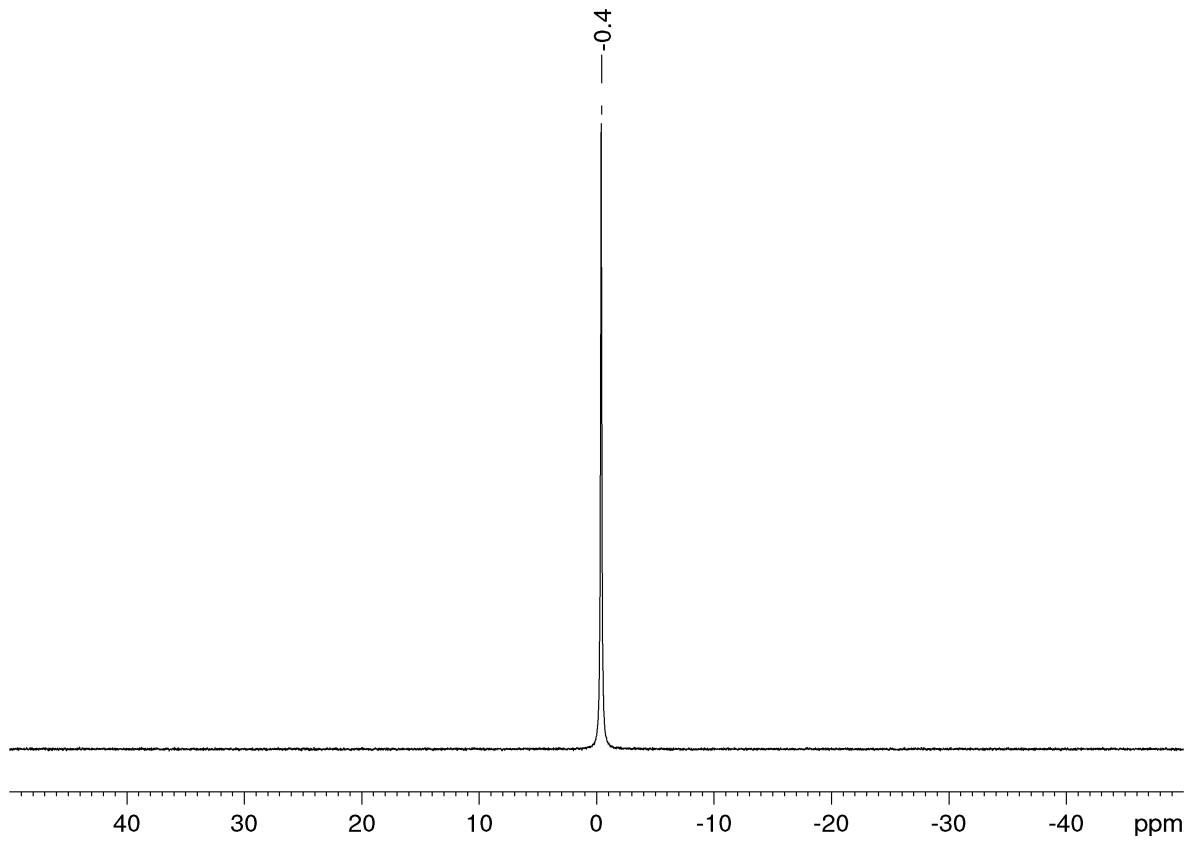

Figure S64. ^{7}Li NMR spectrum (117 MHz) of [Yb(CH_2SiMe_3)$_4$][Li(thf)$_4$] (**6-Yb**) in [D_8]THF at 26 °C.

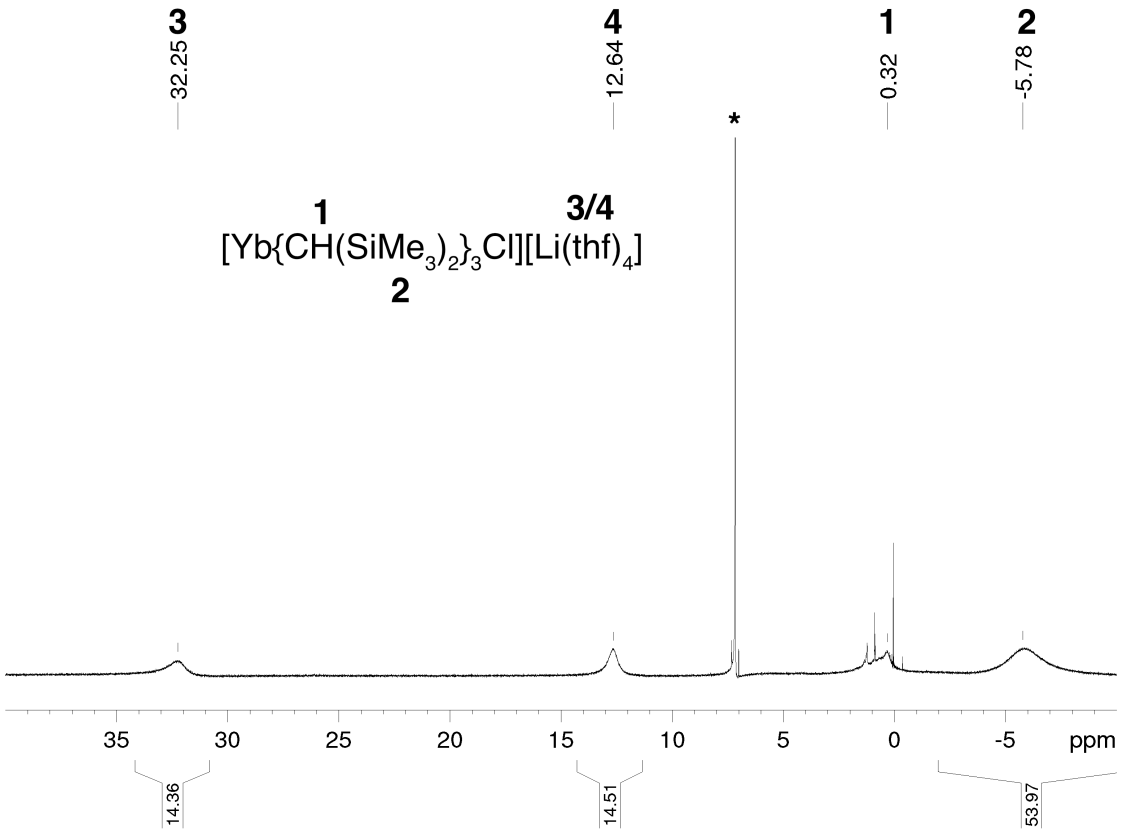

Figure S65. ^{1}H NMR spectrum (500 MHz) of [Yb{$CH(SiMe_3)_2$}$_3$Cl][Li(thf)$_4$] in C_6D_6 at 26 °C. Solvent residual peak is marked with an asterisk.

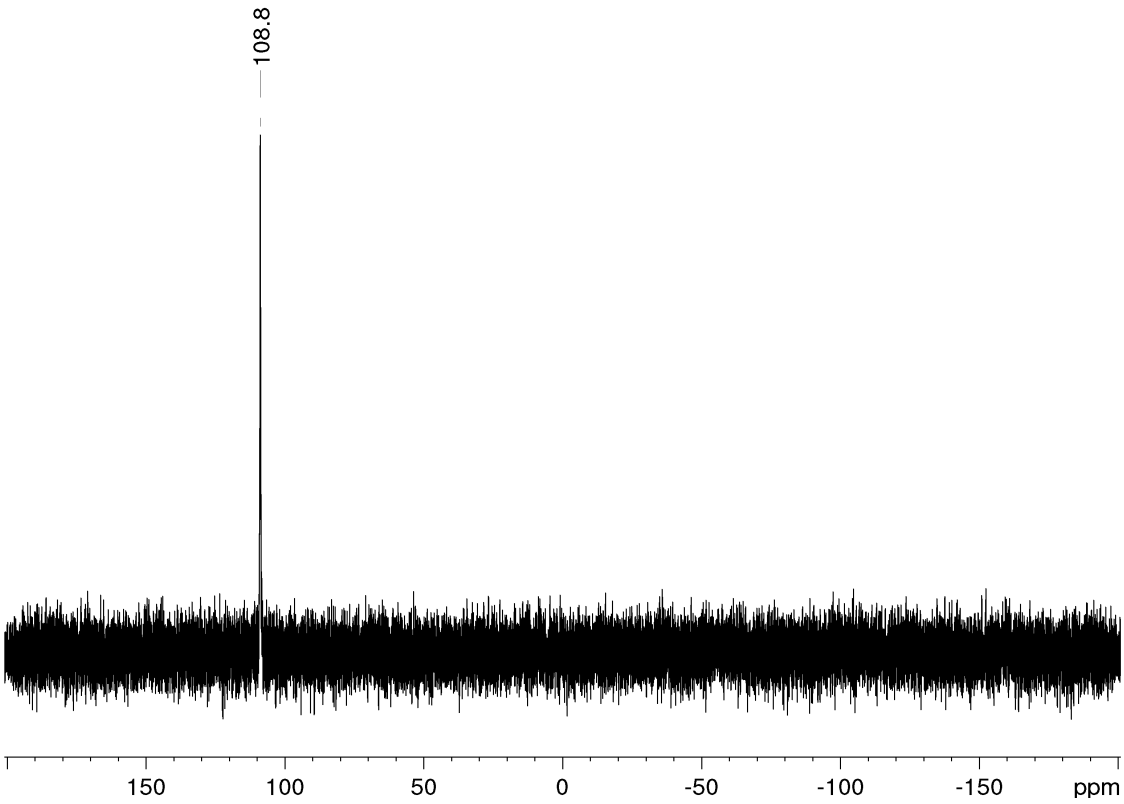

Figure S66. ^{7}Li NMR spectrum (194.4 MHz) of [Yb{CH(SiMe$_3$)$_2$}$_3$Cl][Li(thf)$_4$] in C_6D_6 at 26 °C.

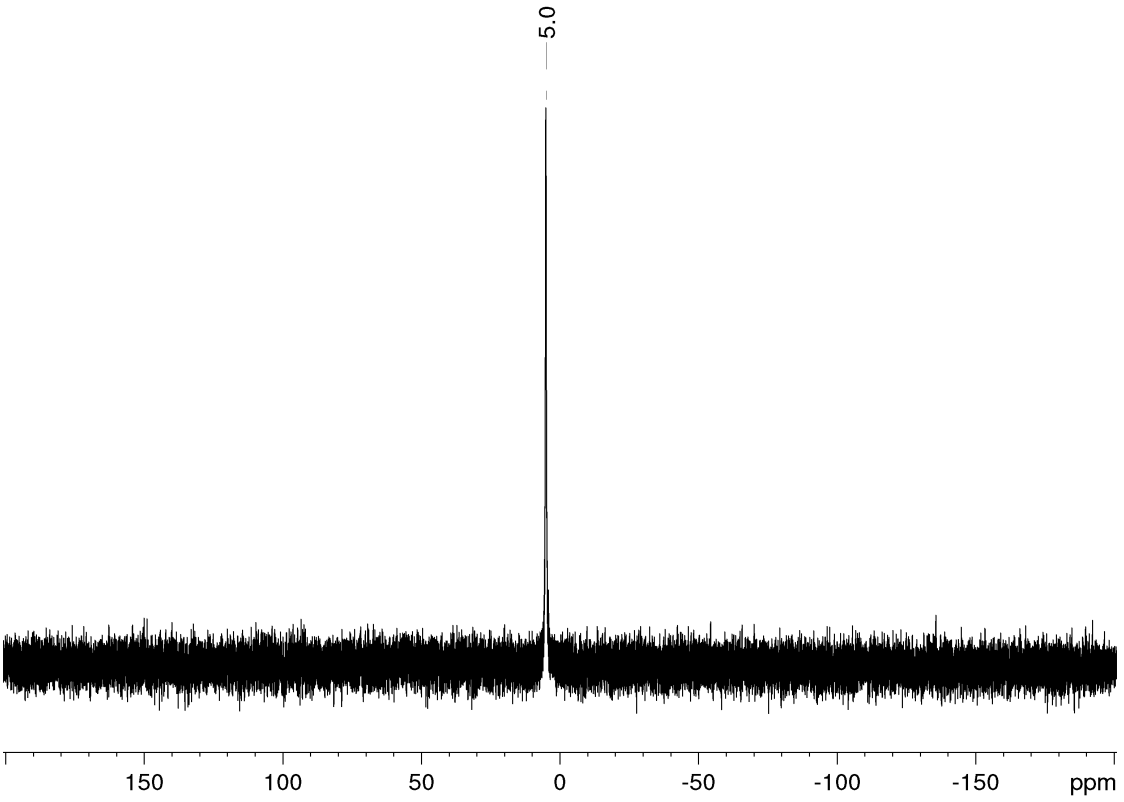

Figure S67. ^{7}Li NMR spectrum (194.4 MHz) of [Yb{CH(SiMe$_3$)$_2$}$_3$Cl][Li(thf)$_4$] in [D_8]THF at 26 °C.

X-Ray Crystallography

Table S1. Crystallographic Data for Compounds 1, 2-Sc, 3, 4, 5 and 7

	1	2-Sc	3	4	5	7
formula	$C_{44}H_{108}Cl_4Li_2O_4Sc_2Si_8$	$C_{33}H_{81}ClLiO_3ScSi_6$	$C_{48}H_{120}Li_2O_4Sc_2Si_8$	$C_{34}H_{84}LiO_3ScSi_6$	$C_{13}H_{33}AlOSi_2$	$C_{79}H_{110}O_6Sc_2$
CCDC	1567519	1990653	1567518	1990652	1567517	1993137
M_r [g mol^{-1}]	1171.62	781.86	1089.96	761.45	288.55	1245.58
color	colourless/block	colourless/ block	colourless/plate	colourless/needle	colourless/ column	colourless/block
crystal dimensions [mm]	0.269 x 0.153 x 0.125	0.285 x 0.153 x 0.134	0.281 x 0.119 x 0.097	0.277 x 0.099 x 0.039	0.252 x 0.144 x 0.140	0.308 x 0.194 x 0.132
cryst syst	triclinic	triclinic[a]	monoclinic	monoclinic	monoclinic	triclinic
space group	$P\bar{1}$	$P\bar{1}$	$P2_1/c$	C2/c	$P2_1/n$	$P\bar{1}$
a [Å]	11.7206(6)	11.9397(19)	13.3428(3)	23.659(4)	16.5825(1)	12.3059(9)
b [Å]	15.8089(9)	12.830(2)	17.6787(4)	12.098(2)	7.2695(5)	13.2573(9)
c [Å]	19.1136(10)	17.909(3)	18.8050(4)	34.338(6)	16.6064(1)	13.4567(10)
α [°]	84.989(3)	96.181(2)	90	90	90	117.844(2)
β [°]	89.272(3)	90.239(2)	125.5710(10)	98.579(4)	109.6080(10)	103.659(2)
γ [°]	79.970(3)	116.570(2)	90	90	90	101.026(2)
V [Å^3]	3474.1(3)	2435.7	3608.05(14)	9718(3)	1885.8(2)	1766.3(2)
Z	2	2	2	8	4	1
T [K]	100(2)	100(2)	100(2)	100(2)	102(2)	173(2)
ρ_{calcd} [g cm^{-3}]	1.120	1.066	1.003	1.041	1.016	1.171
μ [mm^{-1}]	0.519	0.380	0.353	0.326	0.223	0.243
F (000)	1264	856	1200	3360	640	674
θ range [°]	1.620/26.372	2.169/27.095	1.760/27.106	1.199/26.485	2.129/27.877	2.049/30.598
unique reflns	14079	10683	7942	10010	4483	10821
observed reflns (I > 2σ)	9444	7880	6003	6218	3642	9130
R1/*w*R2 (I > 2σ)[b]	0.0447/0.0851	0.0698/0.1995	0.0481/0.1261	0.0561/0.1169	0.0347/0.0819	0.0395/0.1021
R1/*w*R2 (all data)[b]	0.0874/0.0973	0.0892/0.2148	0.0694/0.1406	0.1077/0.1380	0.0485/0.0882	0.0487/0.1091
GOF[b]	1.007	1.070	1.026	0.1018	1.050	1.042

[a] Second modification: monoclinic cell constants for **2-Sc**: a = 12.3944(9) Å,
b = 24.8764(19) Å,
c = 16.8800(12) Å,
β = 96.255(1)°
V = 4867.1 Å^3

[b] $R1 = \Sigma(||F_0|-|F_c||)/\Sigma|F_0|$, $F_0 > 4\sigma(F_0)$. $wR2 = \{\Sigma[w(F_0^2-F_c^2)^2/\Sigma[w(F_0^2)^2]\}^{1/2}$.

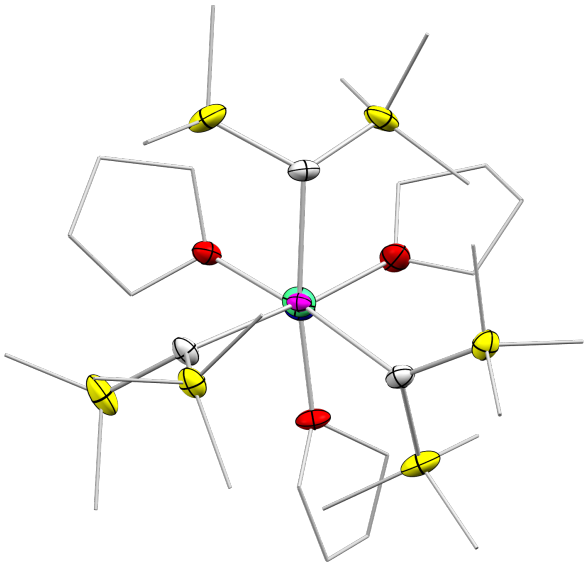

Figure S68. View of the crystal structure of complex **2-Sc** along its Sc–Cl–Li axis.